UCLA
UCLA Previously Published Works

Title

Transintestinal transport of the anti-inflammatory drug 4F and the modulation of transintestinal cholesterol efflux[S]

Permalink

https://escholarship.org/uc/item/4hx5h14k

Journal

Journal of Lipid Research, 57(7)

ISSN

0022-2275

Authors

Meriwether, David
Sulaiman, Dawoud
Wagner, Alan
et al.

Publication Date

2016-07-01

DOI

10.1194/jlr.m067025

Peer reviewed

Transintestinal transport of the anti-inflammatory drug 4F and the modulation of transintestinal cholesterol efflux[S]

David Meriwether,*,† Dawoud Sulaiman,*,§ Alan Wagner,* Victor Grijalva,* Izumi Kaji,*
Kevin J. Williams,† Liqing Yu,** Spencer Fogelman,* Carmen Volpe,†† Steven J. Bensinger,†,§§
G. M. Anantharamaiah,*** Ishaiahu Shechter,* Alan M. Fogelman,* and Srinivasa T. Reddy[1],*,†,†††**

Division of Cardiology, Department of Medicine, David Geffen School of Medicine,* Department of Medical and Molecular Pharmacology,† Molecular Toxicology Interdepartmental Degree Program,§ Department of Microbiology, Immunology and Molecular Genetics,§§ Department of Obstetrics and Gynecology, David Geffen School of Medicine,††† and Division of Laboratory Animal Medicine,†† University of California Los Angeles, Los Angeles, CA; Department of Animal and Avian Sciences,** University of Maryland, College Park, MD; and Department of Medicine,*** University of Alabama at Birmingham, Birmingham, AL

Abstract The site and mechanism of action of the apoA-I mimetic peptide 4F are incompletely understood. Transintestinal cholesterol efflux (TICE) is a process involved in the clearance of excess cholesterol from the body. While TICE is responsible for at least 30% of the clearance of neutral sterols from the circulation into the intestinal lumen, few pharmacological agents have been identified that modulate this pathway. We show first that circulating 4F selectively targets the small intestine (SI) and that it is predominantly transported into the intestinal lumen. This transport of 4F into the SI lumen is transintestinal in nature, and it is modulated by TICE. We also show that circulating 4F increases reverse cholesterol transport from macrophages and cholesterol efflux from lipoproteins via the TICE pathway. We identify the cause of this modulation of TICE either as 4F being a cholesterol acceptor with respect to enterocytes, from which 4F enhances cholesterol efflux, or as 4F being an intestinal chaperone with respect to TICE.[JLR] Our results assign a novel role for 4F as a modulator of the TICE pathway and suggest that the anti-inflammatory functions of 4F may be a partial consequence of the codependent intestinal transport of both 4F and cholesterol.— Meriwether, D., D. Sulaiman, A. Wagner, V. Grijalva, I. Kaji, K. J. Williams, L. Yu, Spencer Fogelman, C. Volpe, S. J. Bensinger, G. M. Anantharamaiah, I. Shechter, A. M. Fogelman, and S. T. Reddy. **Transintestinal transport of the anti-inflammatory drug 4F and the modulation of transintestinal cholesterol efflux.** *J. Lipid Res.* 2016. **57:** 1175–1193.

Supplementary key words atherosclerosis • apolipoprotein A-I mimetic peptides • cholesterol • reverse cholesterol transport

Increasing evidence, both direct and indirect, indicates that the small intestine (SI) may be an important modulator of atherosclerosis. As a result, the SI offers promising therapeutic targets for the prevention and treatment of this disease.

The SI is linked to atherosclerosis in at least four respects. First, intestinal inflammation in the form of inflammatory bowel disease (IBD) has been linked to an increased prevalence of early stage vascular disease in patients without the classical cardiovascular risk factors (1–3). Second, our own recent research has established a link between aberrant levels of lipid signals in the SI and both dyslipidemia and atherosclerosis. Intestinally derived unsaturated lysophosphatidic acids (LPAs) and eicosanoids can both induce dyslipidemia as well as systemic inflammation in LDL receptor null ($LDLR^{-/-}$) mice (4, 5). Dietary LPA can also induce atherogenesis (6), and the levels of unsaturated LPAs in the SI correlate with the extent of atherosclerosis in $LDLR^{-/-}$ mice fed a Western diet (WD) (7).

Third, the SI is an important source of apoAI (8), and at least in mice ∼30% of the steady-state plasma HDL-cholesterol pool is derived from the SI (9). Moreover, while HDL can interrupt atherogenesis by preventing oxidative

modification of LDL (10–13) and promoting reverse cholesterol transport (RCT) from macrophages (14–17), both protective functions of HDL can be lost in a manner that also implicates the SI. During inflammation, HDL proteins and lipids can become oxidatively and enzymatically modified, and HDL can lose its capacity to inhibit LDL oxidation by fatty acid hydroperoxides (18, 19). Intestinal inflammation (3) and aberrant levels of oxidized lipids in the SI (5) can affect this aspect of HDL function. Likewise, the cholesterol efflux capacity of HDL is sensitive to oxidation. For example, the myeloperoxidase (MPO) product hypochlorous acid oxidizes HDL and impairs ABCA1-dependent cholesterol transport (20), and MPO activity is elevated in IBD (21).

Fourth, the intestine itself is directly involved in cholesterol efflux and, together with the luminal reabsorption of cholesterol, the modulation of overall whole body cholesterol load. It is commonly understood that HDL and other lipoproteins return excess peripheral cholesterol to the liver hepatocytes, where the lipoproteins are taken up and transported into the cells. The cholesterol is then converted or secreted into bile and thereby excreted into the intestinal lumen for either reuptake or loss to the feces (22, 23). However, a nonbiliary pathway for cholesterol excretion, known as "transintestinal cholesterol efflux" (TICE), has also been recently identified (24–28). Surgical models involving bile diversion have established that TICE is responsible for ∼33% of total fecal neutral sterol loss in chow-fed C57BL/6J mice (29) and for ∼20% in chow-fed FVB mice (30). Additional studies involving genetic mouse models with severely diminished biliary cholesterol secretion have further confirmed the existence of TICE while also establishing that TICE is a dynamic process that can be stimulated under conditions of biliary insufficiency. For example, Mdr2 P-glycoprotein-deficient mice ($Mdr2^{-/-}$), which are unable to secrete cholesterol into bile, nonetheless have no decrease in fecal neutral sterol loss compared with controls (30). Of particular relevance to this study, mice that highly overexpress human Neiman-Pick C1-like 1 (NPC1L1) in their livers (NPC1L1[-LiverTg112] mice, hereafter Tg112 mice) have <10% of the biliary cholesterol secretion of C57BL/6J controls, but they have no decrease in fecal neutral sterol levels. As these mice also exhibit no difference in intestinal cholesterol absorption, TICE must account for the bulk of the sterol excretion into the feces in these mice (31, 32).

Increasing cholesterol efflux through the intestine might lower LDL cholesterol (LDL-C) directly, potentially amplifying the atheroprotective effects of statins and cholesterol uptake inhibitors (33). Targeting TICE also raises the possibility of enhancing RCT itself (28). Moreover, selectively targeting TICE would avoid the side effect of gallstones that could come from modulating RCT by increasing biliary cholesterol secretion (34). Alternatively, targeting intestinal inflammation and oxidized lipids in the SI holds promise as a treatment for atherosclerosis, for the reasons elucidated above.

The apoAI mimetic peptide 4F is an 18 amino acid amphipathic helix 4F that has the structure Ac-D-W-F-K-A-F-Y-D-K-V-A-E-K-F-K-E-A-F-NH$_2$ (35). 4F synthesized from L-amino acids (L-4F) and from D-amino acids (D-4F) has been used in biological studies. D-4F and L-4F were shown to have the same in vitro and in vivo properties, indicating that stereospecificity is not essential to the activity of the peptide (36, 37).

4F has been shown to be effective as a treatment for atherosclerosis in numerous animal models (38, 39). 4F has also been shown to improve HDL function (40, 41), reduce systemic inflammation (42), reduce oxidative stress (43), and increase the clearance of oxidized lipid species from the circulation (44). Given these effects, and given the nature and location of atherosclerosis itself, our laboratory had long assumed that the circulation was the site of action for 4F (45). However, when we investigated the relationships between mode of administration, plasma levels, and efficacy of the drug, we discovered that the plasma levels of 4F did not in fact determine its efficacy (46). Both oral and subcutaneous (SQ) D-4F at doses of 4.5 and 45 mg/kg significantly improved markers of HDL function and systemic inflammation equally for a given dose, but these modes of administration achieved very different plasma levels of peptide, with SQ levels being ∼1,000× higher. Rather, the equally effective SQ and oral doses achieved equal concentrations of 4F only in the feces (46) and the SI (5). This finding suggested that the intestine may be the site of action for 4F. Of note, the second study further established that both SQ and oral D-4F lowered the levels of oxidized signaling lipids in the SI while simultaneously improving markers of HDL function and systemic inflammation (5).

Our prior work did not further investigate whether and in what manner circulating 4F targets the SI. This current study thus began as a mechanistic pharmacokinetic investigation into the distribution and excretion of intravenously administered and circulating 4F as regards the SI. We have here determined that circulating 4F selectively targets the proximal SI and is largely transported into the intestinal lumen in a transintestinal manner. We have further observed that lumen-side 4F can be taken back up into intestinal tissue, suggesting the possibility of cycling or recirculating 4F through both lumen and tissue.

TICE also selectively targets the proximal SI (28), and lipoproteins including VLDL and LDL (48) and possibly HDL (49) are sources of the cholesterol effluxed through the TICE pathway. We have previously shown that circulating 4F has a high affinity for HDL and other lipoproteins (44), as well as for cholesterol (50). Thus, we next hypothesized that the transintestinal transport of 4F might partially depend on the transintestinal efflux of cholesterol. Using the genetic Tg112 mouse model and ex vivo studies involving Ussing chambers, we have discovered that the transport of 4F into the intestinal lumen is partially mediated by TICE.

Interestingly, when we investigated the converse, whether 4F and 4F secretory transport can themselves modulate cholesterol efflux, we observed that circulating 4F can increase RCT from macrophages and cholesterol efflux from lipoproteins in Tg112 mice. We further observed ex vivo that 4F can increase the transintestinal

efflux of cholesterol across duodenal explants. Together, these data indicate that 4F can modulate cholesterol excretion via the TICE pathway. As such, we here report on a novel means of increasing TICE while also adding detail regarding the intestinal-specific mechanism of the anti-inflammatory and antiatherogenic drug 4F.

MATERIALS AND METHODS

ApoA-I mimetic peptide 4F

The amino acid sequence of 4F is Ac-D-W-F-K-A-F-Y-D-K-V-A-E-K-F-K-E-A-F-NH$_2$. 4F was synthesized from L-amino acids (L-4F) and D-amino acids (D-4F) by the solid phase peptide synthesis method previously described (51, 52). During the peptide chain elongation the ε-amino groups of the lysines were protected by t-butyloxy-carbonyl (t-BOC). The final step for the cleavage of the peptide from the resin along with the cleavage of t-BOC protecting groups was accomplished using trifluoroacetic acid with suitable scavengers. Under these conditions, the N-terminal acetyl group is stable, whereas all of the other t-butanol protecting groups are cleaved. For synthesizing ^{14}C-peptide, ^{14}C-acetic anhydride was used instead of acetic anhydride as previously described (53). Peptide purity was ascertained by mass spectral analysis and analytical HPLC. L-4F, D-4F, and carbon-14-labeled L-4F (^{14}C-L-4F), as well as 4F-internal standard (IS) (^{15}N,^{13}C-4F), were synthesized in the laboratory of G. M. Anantharamaiah at the University of Alabama.

Mice, diets, and treatments

WT C57BL/6J mice were obtained from the breeding colony of the Department of Laboratory and Animal Medicine at the David Geffen School of Medicine at University of California Los Angeles (UCLA) after having been originally purchased from Jackson Laboratories. NPC1L1$^{-LiverTg112}$ mice (Tg112 mice) were developed and supplied by the laboratory of Liqing Yu (31). All mice were maintained on a chow diet (Ralston Purina) unless otherwise noted. WD (Harlan-Teklad TD.88137) consisted of 0.2% cholesterol and 21% total fat. For the studies involving WD, mice were fed WD for 6 weeks prior to the experiments. Liver X receptor (LXR) agonist treatment consisted of T0901317 (Cayman 71810) suspended in a vehicle containing 1.0% carboxymethylcellulose and 0.1% tween 80. Mice were gavaged with 25 mg/kg T0901317 once daily for a period of 7 days (32). For all experiments, approximately equal numbers of male and female mice were used. All experiments were performed using protocols approved by the Animal Research Committee at UCLA and in conformity with the Public Health Service Policy on Humane Care and Use of Laboratory Animals.

Isolation of lipoproteins from human plasma

Healthy human donor subjects were recruited after written consent approved by Institutional Review Board at UCLA. Fasting blood was collected in heparinized tubes (Becton Dickinson), and the plasma was separated by centrifugation. Human LDL and HDL were isolated by density centrifugation and were obtained from the Atherosclerosis Research Unit Core facility. LDL was isolated between densities of 1.019 and 1.063 g/ml, and HDL between densities of 1.063 and 1.21 g/ml. After isolation, the lipoproteins were dialyzed to remove the added salts (54).

Determination of radioactivity

Radioactivity was determined as dpm by scintillation counting in 10.0 ml BioSafe II scintillation fluid (RPI Corporation) on a Packard Tri-Carb Model A900TR using QuantaSmart software.

LC/MS/MS analysis

LC/MS/MS was performed using a 5500 QTRAP quadruple mass spectrometer (SCIEX) equipped with electrospray ionization source. The HPLC system utilized an Agilent 1290 series LC pump equipped with a thermostatted autosampler (Agilent Technologies). Chromatography was performed using YMC-Pack ODS-AQ column (3 μm particle, 50 × 2.0 mm; YMC) with a security guard cartridge at 45°C. Mobile phase A consisted of 0.1% formic acid in water, and mobile phase B consisted of 0.1% formic acid in acetonitrile. The autosampler was set at 4°C. The injection volume was 10 μl, and the flow rate was controlled at 0.2 ml/min. The gradient program was as follows: 0–12 min, linear gradient from 5% to 95% B; 12–14 min, 95% B; 14–14.5 min, linear gradient to 5% B; 14.5–20 min, 5% B. The data acquisitions and instrument control were accomplished using Analyst 1.6.2 software (SCIEX). Detection was accomplished by using the multiple reaction monitoring mode with positive ion detection; the parameter settings used were as follows: ion spray voltage = 5,500 V; curtain gas = 10 (nitrogen); ion source gas 1 = 60; ion source gas 2 = 70; temperature = 500°C. Collision energy, declustering potential, and collision cell exit potential were optimized for each compound to obtain optimum sensitivity. The transitions monitored were for m/z 578.6/103.1 and 578.6/120 for both L-4F and D-4F, and 581.8/84.2 for 4F-IS (^{15}N,^{13}C-4F). Quantification was performed relative to IS using Analyst 1.6.2.

GC/MS analysis

Derivitized sterol samples in pyridine and N,O-Bis (trimethylsilyl) trifluoroacetamide with trimethylchlorosilane (BSTFA + TMCS) reagent were run on an Agilent 7890B/5977A with a ZB-MR1 column (Zebron 7HG-G016-11). One microliter of sample was injected in split mode. Full oven program and MS settings are available upon request (55). MS detector was run in SIM mode. For in vivo studies involving analysis of fecal neutral sterols, fecal neutral sterol mass represents the sum of cholesterol, coprostanol, and coprostanone in each sample (56). IS 5α-cholestane was detected by parental ion of m/z 372. The TMS forms of coprostanol, cholesterol, and coprostanone were identified by RT relative to standards as well as by parental ions m/z 460.4, 458.4, and 458.4 respectively. Quantification was by the ratio of area under the curve (AUC) of parental ions to AUC of IS, relative to the parental ion to IS ion ratios of the appropriate standard curves. For the ex vivo study involving analysis of cholesterol alone, the IS stigmastanol was detected by the TMS form at m/z 488.4, while cholesterol was detected by the cholesterol TMS fragment at 329.4.

Sample preparation for MS analysis

For LC/MS/MS analysis of 4F in mucosal media, IS was added to mucosal media, and the media was injected directly into the LC/MS/MS without further sample preparation. 4F was extracted from tissue and from SI rinse using the method of Bligh and Dyer (57) following addition of IS, and upon concentration the aqueous phase was injected directly into the LC/MS/MS. For GC/MS analysis of neutral sterols in feces, cage feces were dried overnight at 50°C . Approximately 100 mg of feces was isolated, crushed into a fine powder, and weighed exactly. Fifty micrograms of 5α-cholestane was added. Sterols were first saponified in 2 ml of ethanol, together with 200 μl of 50% (w/v) KOH, and the mixture was homogenized and heated at 65°C for 2 h. One milliliter of deionized water was added, and then sterols were extracted twice into 2 ml of n-hexane (58). Two hundred microliters of hexane from the combined extractions was dried down, and samples were derivatized by adding 50 μl of anhydrous pyridine (Sigma, 270970) and 50 μl of BSTFA + TMCS, 99:1 (Sigma,

33155-U). For determination of fecal neutral sterols in the feces of individual mice, ~10–20 mg of feces was isolated from the distal colons of mice before being dried, weighed, and treated as above. For determination of cholesterol in mucosal media from the Ussing chamber experiments, 2 µg of stigmastanol was first added to 1 ml of media, the sterols were extracted using the method of Folch (59), and samples were further treated as above.

4F distribution studies

4F (L-4F, D-4F, or ~0.2 µCi ^{14}C-L-4F) was administered at 25 mg/kg via tail vein. At predetermined time points between 3 and 60 min, the animals were euthanized and perfused, and organs were dissected. Organs were homogenized, and ^{14}C-L-4F was determined by scintillation counting, while both L-4F and D-4F were determined by LC/MS/MS.

In vivo 4F secretory transport studies

In order to assess whether circulating 4F was transported into the intestinal lumen, C57BL/6J mice were iv administered 25 mg/kg ^{14}C-L-4F (~2.0 µCi) via tail vein. After 1 or 3 h, the animals were bled, euthanized, and perfused. The entire SI from stomach to cecum was dissected, before being sequentially rinsed three times using PBS, 0.6% taurocholate, and 1.0% Triton-X 100. The rinses were collected and combined for analysis. Large intestine was dissected and washed with PBS three times, while the contents of the gall bladder were collected via insulin syringe. Tissues were dissected and homogenized prior to analysis. Radioactivity was determined in all samples via scintillation counting. This experiment was then repeated with L-4F, with the SI wash consisting only of 3× PBS, and analysis being performed via LC/MS/MS. High-dose (100 mg/kg) and low-dose (25 mg/kg) secretory transport studies in C57BL/6J were performed similarly. The effect of WD on the secretory transport of 4F was studied in Tg112 mice by first feeding the animals with WD or chow for 6 weeks. Then 25 mg/kg ^{14}C-L-4F was injected via tail vein, and radioactivity in SI rinse was determined as above. Feces from these individual mice were collected directly from the distal colon of these mice, and levels of neutral sterols in the feces were determined by GC/MS (56).

Bile duct ligation study

C57BL/6J mice were anesthetized with isoflurane (5% induction, 1–2% maintenance), and bile ducts were either ligated or sham ligated. We validated our surgical technique in a pilot study by monitoring Alcian blue that had been injected directly into the gall bladder: ligated mice showed no passage of Alcian blue into the duodenum. Because of the constraints of our surgical protocol, as well as our interest in observing the transport of intact peptide, we then injected 25 mg/kg L-4F (rather than ^{14}C-L-4F) via tail vein into both ligated and sham-ligated mice; after 1 h, we determined L-4F in intestinal PBS rinse using LC/MS/MS.

Lung lavage

In order to study the transport of 4F into the alveolar space, ^{14}C-L-4F was iv administered to C57BL/6J mice at both t = 0 h and t = 3 h. At t = 4 h, the mice were euthanized. The lungs and trachea of the mice were exposed by cutting longitudinally along the sternum, being careful to avoid damaging the lungs or trachea. A needle (20G, Fisher) was introduced into the proximal portion of the trachea, parallel with the trachea. Once secured, a 3 ml syringe (Fisher) filled with 1.3 ml PBS was attached to the needle, and the lung was flushed three times, allowing for the total volume to fill the lung with each flush. The lavage fluid was collected, and the procedure was repeated 3 to 4 times for a total of 5 ml/mouse (60). ^{14}C-label was determined in the wash by scintillation counting.

Ussing chamber studies: general

Ussing chamber experiments were carried out in an Easy-Mount Ussing Chamber System (EM-CSYS-2-Physiologic Instruments). For all studies, duodenal explants (muscle on) from C57BL/6J mice, 8–10 weeks of age, were mounted on sliders (P2304-Physiologic Instruments). Once in the Ussing Chambers, intestinal explants were incubated at 37°C. The serosal and mucosal chambers contained 4 ml Krebs-Ringer buffers that were gassed at 95% O_2, 5% CO_2 (serosal bath), and 100% O_2 (mucosal bath). The Krebs-Ringer buffers were at pH 7.4 after initial gassing with 95% O_2, 5% CO_2; they had the following composition: 115 mM NaCl, 25 mM NaHCO$_3^-$, 2.4 mM K$_2$HPO$_4$, 1.2 mM CaCl$_2$, 1.2 mM MgCl$_2$, 0.4 mM KH$_2$PO$_4$, with 10 mM glucose and 10 mM mannitol added in the serosal and mucosal buffers, respectively (61). The Ussing chamber runs lasted 90 min, and 500 µl samples were taken from each chamber every 0, 30, 60, and 90 min. Unless otherwise noted, all mucosal chambers also contained 1× micelles, in accord with the preparation of Iqbal et al., 0.14 mM sodium cholate, 0.15 mM sodium deoxycholate, 0.17 mM phosphatidylcholine, 1.2 mM oleic acid, and 0.19 mM monopalmitoylglycerol (62). Where indicated, serosal chambers contained human LDL and HDL at 0.72 mg protein/ml and 0.174 mg protein/ml, respectively. Nonpermeable 70 kDa FITC-dextran beads (Sigma Aldrich) were utilized to determine intestinal explant integrity by observing their absence in the mucosal chamber when added into the serosal chamber from 90 to 100 min (49).

Ussing chamber studies: 4F uptake and secretory transport

For in vivo-ex vivo 4F secretory transport studies, 800 µg (~25–30 mg/kg) of D-4F or L-4F in 300 µl saline was injected via tail vain into C57BL/6J mice. After 30 min, the mice were euthanized, and duodenal explants were mounted in Ussing chambers as above. Serosal chambers either did or did not contain HDL + LDL, while mucosal chambers contained 1× micelles. 4F in both tissue and mucosal media was determined by LC/MS/MS, while cholesterol in mucosal media was determined by GC/MS. The levels of 4F in mounted tissues were compared with the levels of 4F in matching pieces of duodenum that had been taken from the same mice but that had not been mounted. For ex vivo 4F uptake studies, duodenal explants from C57BL/6J mice were mounted in Ussing chambers. Fifty micrograms per milliliter of L-4F alone was added to the mucosal chambers. After 90 min, the explants were removed and washed 3× in PBS. Uptake of 4F by the tissue was determined by LC/MS/MS. Fifty micrograms per milliliter of ^{14}C-L-4F was added to the serosal chambers of additional explants. Again after 90 min, the tissue was washed 3×, and uptake of 4F by the tissue was determined by scintillation counting.

Ussing chamber studies: TICE

In the in vivo-ex vivo TICE study, to investigate the effect of 4F on TICE within our Ussing chamber system, C57BL/6J mice were first injected with 800 µg D-4F (~25–30 mg/kg) via tail vein. After 30 min, the animals were euthanized, and explants were mounted in Ussing chambers as above. Each 4F-loaded explant had a sham-injected control explant that was run simultaneously and under identical conditions. Serosal media contained ^{3}H-cholesterol-loaded LDL and HDL, while mucosal media contained 1× micelles. ^{3}H-label was determined in both tissue and mucosal media by scintillation counting. In the ex vivo TICE study, duodenal explants from C57BL/6J mice were mounted in Ussing chambers as above. Serosal media contained ^{3}H-labeled LDL + HDL, prepared as below, while mucosal media contained 0.25× micelles with or without 50 µg/ml D-4F. ^{3}H-label was determined in

both mucosal media and tissue after 90 min. For both of these studies, D-4F rather than L-4F was used in order to sidestep the possibility of loss of peptide function due to proteolysis across the 90 min of the Ussing chamber incubations.

J774 cell culture and ^{3}H-cholesterol loading

J774 mouse macrophages were grown in RPMI-1640 medium supplemented with 10% FBS, 100 U/ml penicillin, and 100 µg/ml streptomycin. Cells were incubated with 5 µCi/ml ^{3}H-cholesterol (cholesterol [7-3H(N)], ARC) and 100 µg/ml acetylated LDL for 48 h. Prior to injection, the resulting foam cells were washed, equilibrated, harvested, and resuspended in media without FBS. All cell suspensions were analyzed microscopically to determine the number of live cells, and radioactivity was determined as above. On average, injections consisted of 2×10^6 cells and 1 µCi ^{3}H-cholesterol.

In vivo macrophage RCT studies in Tg112 and WT mice

The investigation of macrophage RCT in Tg112 and WT mice was performed in accord with the Rader group protocol (63), except that we measured cholesterol efflux into the SI lumen rather than sterol excretion into the feces (32). At t = 0 h, mice were injected intraperitoneally with ∼500 µl of ^{3}H-cholesterol labeled foam cell suspension. After 8 h, the mice were euthanized, and luminal rinse was collected. The rinse was then subjected to chloroform/methanol extraction by adding 4.5 ml of chloroform-methanol (2:1, v/v) to 2 ml of the lumen PBS rinse (32). Following centrifugation, the lower chloroform phase containing ^{3}H-cholesterol was collected, dried, and resuspended in scintillation cocktail for determination of radioactivity. The upper aqueous phase containing ^{3}H-bile acids was added directly to scintillation cocktail for determination of label. In order to study the effect of circulating 4F on cholesterol efflux in this model, 25 mg/kg ^{14}C-L-4F was intravenously administered at t = 4 h and again at t = 7 h. At t = 8 h, SI rinse was collected and ^{3}H-cholesterol was determined, and ^{14}C label was determined directly in PBS rinse. ^{14}C-L-4F and scintillation counting, rather than L-4F and LC/MS/MS, were used in this study to determine peptide levels in order to avoid the possibility of tritium contamination of the LC/MS/MS.

In vivo cholesterol efflux studies in Tg112 and WT mice

Human HDL and LDL were labeled by adding ethanol-suspended ^{3}H-cholesterol directly to the lipoprotein mix and then removing any precipitate by centrifugation. For each mouse, 2 µCi ^{3}H-cholesterol was combined with 0.1 mg HDL cholesterol and 0.1 mg LDL-C. Labeled lipoprotein was then premixed with ^{14}C-L-4F (25 mg/kg/mouse) or vehicle before injection by tail vein into both Tg112 and littermate control mice. At t = 3 h, an additional 25 mg/kg ^{14}C-L-4F or vehicle was injected into each mouse. After 4 h, the mice were euthanized and processed as above. As before, ^{14}C-L-4F and scintillation counting, rather than L-4F and LC/MS/MS, were used in this study to determine peptide levels in order to avoid the possibility of tritium contamination of the LC/MS/MS.

Primary enterocyte cholesterol efflux study

Primary enterocytes were extracted and loaded with ^{3}H-cholesterol following the method of Iqbal et al. (62) C57BL/6J mice were fasted overnight and then euthanized. SI was removed by dissection. Contents from the intestinal lumen were removed, washed with 117 mM NaCl, 5.4 mM KCl, 0.96 mM NaH$_2$PO$_4$, 26.19 mM NaHCO$_3$, and 5.5 mM glucose, and then filled with 67.5 mM NaCl, 1.5 mM KCl, 0.96 mM NaH$_2$PO$_4$, 26.19 mM NaHCO$_3$, 27 mM sodium citrate, and 5.5 mM glucose (buffer A).

Intestines were bathed in oxygenated saline at 37°C for 10 min. After discarding the buffer, the intestinal lumen was refilled with buffer A containing 1.5 mM EDTA and 0.5 mM DTT and incubated in 0.9% sodium chloride solution at 37°C for 10 min. Luminal contents were collected and centrifuged at 1,500 rpm for 5 min. All buffers were adjusted to pH 7.4, gassed with 95% O$_2$/5% CO$_2$ for 20 min, and maintained at 37°C prior to use. Enterocytes were then suspended in 1.5 ml DMEM containing ∼1 µCi/ml ^{3}H-cholesterol and incubated at 37°C. Cells were gassed with 95% O$_2$/5% CO$_2$ every 15 min. After 1 h, enterocytes were centrifuged and washed three times with DMEM before being incubated with vehicle, micelles, or L-4F. After 2 h, the cells were pelleted and ^{3}H-label was determined in the supernatants by scintillation counting.

Statistical analyses

Error is reported throughout as ± SEM. Statistical analyses were performed by unpaired two-tailed Student's t-tests, except where experimental groups were paired with matched controls, in which cases analyses were performed by paired two-tailed t-tests. Significance was set at $P < 0.05$.

RESULTS

4F that is introduced directly into the circulation preferentially associates with the proximal small bowel

In order to investigate the distribution of circulating 4F, we first administered 25 mg/kg ^{14}C-L-4F to C57BL/6J mice (n = 3) via tail vein. We observed that peptide label selectively targeted the SI 60 min postinjection (**Fig. 1A**). In order to determine the kinetics of 4F uptake by the intestine, we examined the accumulation of 4F label at multiple time points from 3 to 60 min. We observed that both the duodenum and the jejunum but not the ileum or colon showed significant uptake of label across 0–60 min ($P = 0.003$ and 0.001, respectively), with duodenal uptake peaking at 15–30 min (Fig. 1B). Next, in order to rule out the possibility that we had observed the uptake of mere label rather than intact peptide, we intravenously administered 25 mg/kg L-4F (Fig. 1C) and D-4F (Fig. 1D), and we determined at 15 min postinjection the intestinal distribution of intact peptide by LC/MS/MS. We here observed similar patterns of distribution for L-4F and D-4F at 15 min as for ^{14}C-L-4F at both 15 and 60 min, indicating that the prior apparent uptake of 4F by the duodenum and jejunum but not ileum was neither the result of proteolysis nor clearance by the jejunum. Approximately 7.5% of total injected L-4F and D-4F was present intact in the duodenum and jejunum, but the concentrations of L-4F and D-4F were significantly higher for both in the duodenum compared with the jejunum ($P = 0.001$ and 0.005, respectively), indicating that both circulating L-4F and D-4F selectively target the proximal small bowel. The concentration of D-4F in both the ileum and cecum was higher than that of L-4F, likely indicating that at least some proteolysis of L-4F in the distal SI had taken place. However, both intravenously administered L-4F and D-4F behaved comparably as regards distribution from the circulation to the SI.
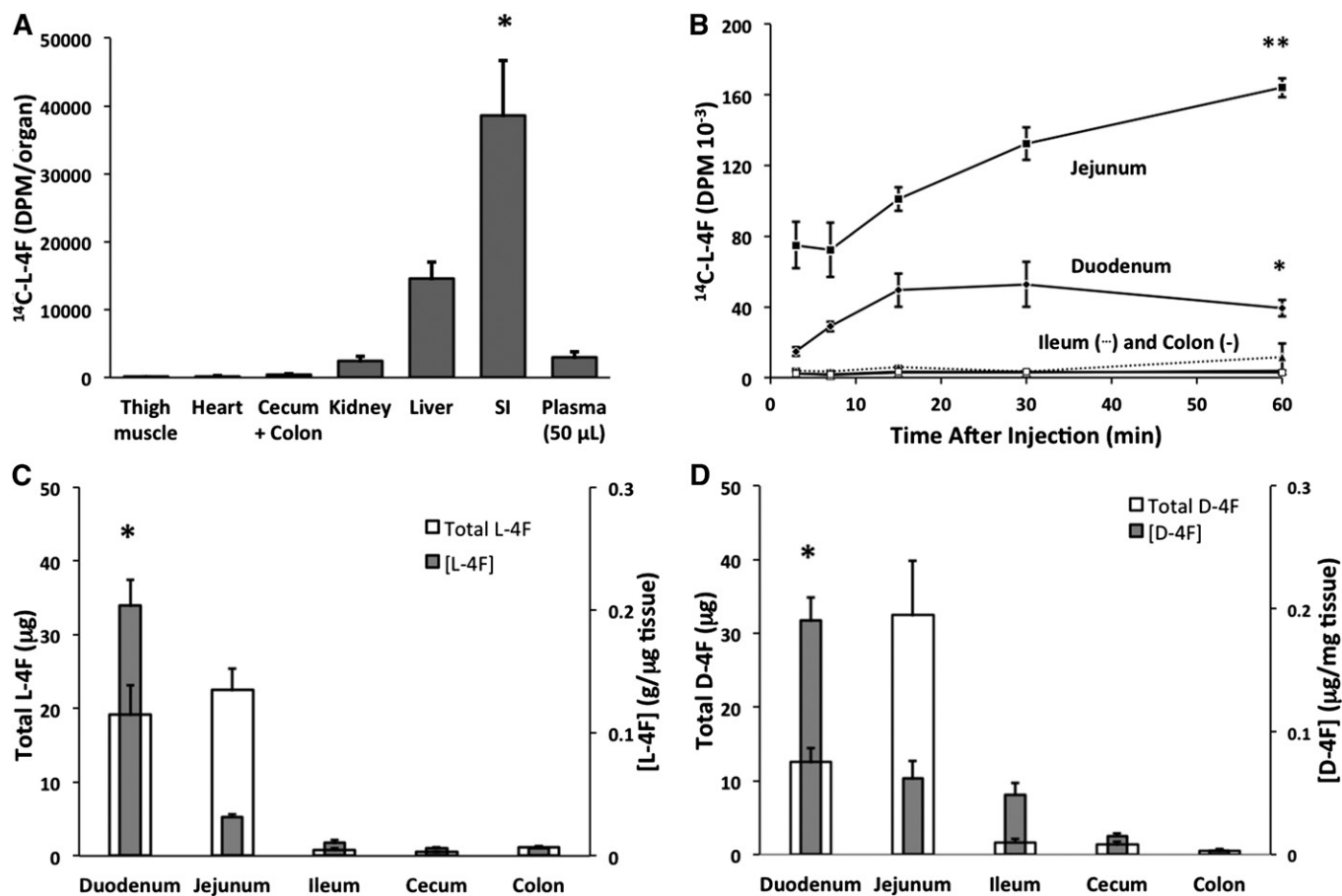
Fig. 1. L-4F that is introduced directly into the circulation preferentially associates with the proximal small bowel. A: Gross tissue distribution was first determined by injecting ^{14}C-4F (25 mg/kg, 0.2 μCi) into C57BL/6J mice via the tail vein (n = 3). After 60 min, the mice were euthanized and perfused, tissues were dissected and homogenized, and radioactivity was determined by scintillation counting. Counts were significantly higher in the SI compared with the liver (* P = 0.04). B: ^{14}C-L-4F (25 mg/kg, 2 μCi) was injected via tail vein directly into the circulation of each of 15 fasted C57BL/6J mice. At various time points, the animals were euthanized, perfused, and dissected, and radioactivity was determined (3 mice/time point). A significant increase in radioactivity between 3 and 60 min was observed for both the duodenum (* P = 0.003) and the jejunum (** P = 0.001). C, D: L-4F or D-4F (25 mg/kg) was injected via tail vein into C57BL/6J mice (n = 4 per peptide). After 15 min, the animals were euthanized and perfused, and levels of intact peptide were determined in intestinal tissue via LC/MS/MS. Both peptides exhibited distribution patterns comparable to each other and to that at 15 min and 60 min in B. The concentrations of intact L-4F and D-4F were both significantly higher in the duodenum compared with the jejunum (* P = 0.001 and P = 0.005, respectively). Error is reported as SEM.

Circulating 4F that associates with the SI is transported into the SI lumen by directly and selectively crossing the intestinal epithelium

In the experiments described above (Fig. 1), we perfused the mice but did not clear the small intestinal contents before determining the distribution pattern of 4F. We next sought to determine with what radial compartment of the SI—lumen, mucosa, submucosa, muscle, or serosa—4F associated. In pilot experiments, we intravenously administered 25 mg/kg ^{14}C-L-4F into C57BL/6J mice, and after 1 h, we euthanized and perfused the animals (n = 3). We freed the lumen of chyme, tied off and filled the SI with a lower-salt buffer followed by a high-salt buffer containing EDTA and DTT, and thereby isolated enterocytes (64). We observed that the label was largely present in the first buffer rather than in enterocyte fraction or in the remaining tissue (data not shown), suggesting that 4F had been transported into the SI lumen. We then intravenously

administered 25 mg/kg ^{14}C-L-4F (1.8 μCi) into C57BL/6J mice; at the end of 1 or 3 h (n = 3 mice/time point), mice were euthanized and perfused. We collected and determined radioactivity in a series of rinses of the SI: PBS alone, followed by a rinse of simple taurocholate micelles in order to penetrate the mucin layer (65, 66), followed by a rinse of 1% Triton X-100 in order to dissolve the cell membranes of the mucosa (67). We further analyzed the remaining intestinal tissues, as well as the liver and contents of the gall bladder (**Fig. 2A**). Approximately 66% of the label associating with the SI was present in the PBS rinse by 1 h, with no further label added by 3 h. After 3 h, label associated with the SI rinses and SI tissue had decreased by 33% from ∼260,000 dpm to 170,000 dpm, while label present in the cecum and contents had increased 20-fold from 4,000 to 80,000 dpm, indicating that label that had been released into the lumen by 1 h was traversing the SI to the cecum. Label was also present in

the feces by 3 h. In addition, label was found in the liver and the contents of the gall bladder, with gall bladder label increasing ~2-fold from 1 to 3 h. In order to confirm that the results of Fig. 2A were for intact peptide and not merely peptide label, we repeated the 1 h time point experiment described in Fig. 2A using L-4F; we determined by LC/MS/MS that ~5% of total injected peptide was present intact in the initial PBS rinse (Fig. 2B).

The data of Fig. 2A are consistent with 4F reaching the SI lumen both transintestinally and through the hepatobiliary pathway. Consistent with label loading the SI tissue from the circulation before being released directly into the lumen, label was present in both the Triton X-100 rinse and in the remaining SI tissue homogenate, with this label decreasing over time. However, consistent with 4F
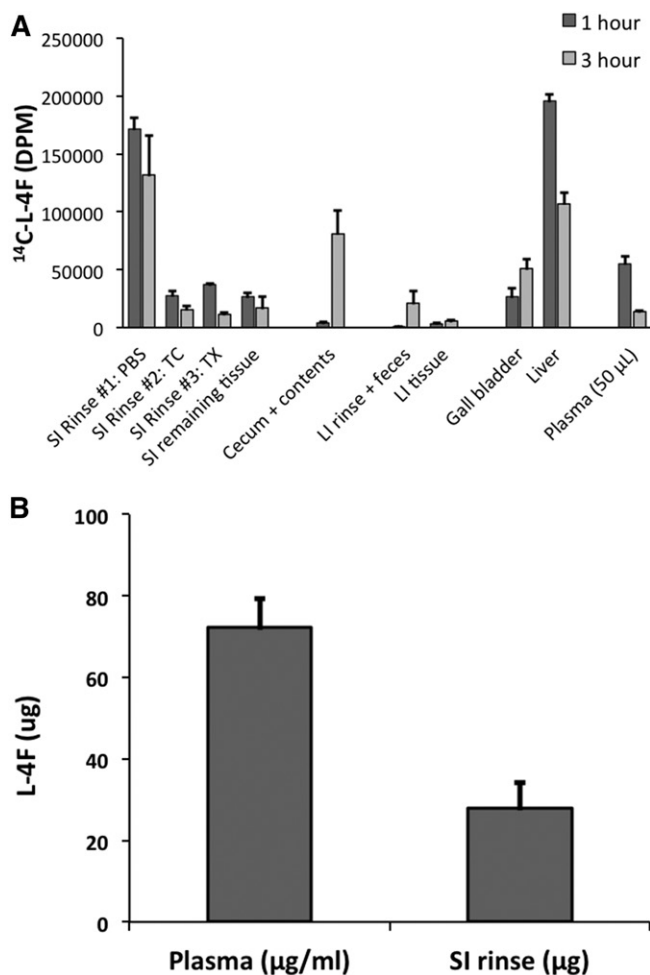

Fig. 2. Small intestinal 4F is transported into the intestinal lumen. A: ^{14}C-L-4F (25 mg/kg, 1.8 μCi) was introduced via tail vein into the circulation of fasted male C57BL/6J mice. After 1 or 3 h (3 mice/time point), the animals were bled, euthanized, perfused, and dissected. The entire SIs were then rinsed three times with PBS, followed by three times with 0.6% taurocholate (TC) and three times with 1.0% Triton X-100 (TX). Radioactivity was determined in all of the rinses as well as in associated tissues, cecum contents, feces, and gall bladder contents (Gall bladder). B: Intact L-4F present in SI PBS rinse was determined by LC/MS/MS after 1 h following tail vein injection of L-4F (25 mg/kg) into C57BL/6J mice (n = 4). Error is reported as SEM.

entering the lumen through the hepatobiliary pathway, label was also present in the contents of the gall bladder. While label in the gall bladder increased during the same time window in which label in the SI lumen was decreasing, suggesting a transintestinal pathway for 1 h luminal 4F, there nonetheless exist reports that some lipophilic peptides are excreted into the SI lumen through the liver and bile (68). Thus, in order to investigate the path by which 4F enters the SI lumen, we ligated the bile ducts of C57BL/6J mice and compared the amount of intact L-4F in the luminal PBS rinse of ligated animals compared with sham-ligated controls. We first validated our surgical procedure by injecting Alcian blue into the gall bladders of both ligated and sham-ligated mice and showed that blue dye entered the duodenum only in sham-ligated animals (supplementary Fig. 1A, B). Next, we intravenously administered 25 mg/kg L-4F to both ligated and sham-ligated mice (n = 3 mice/group), euthanized the animals after 1 h, and determined the levels of intact L-4F in the SI rinse by LC/MS/MS. We observed no difference in 4F transport between ligated and sham-ligated mice ($P = 0.5$) (**Fig. 3A**), showing that under these conditions L-4F enters the SI lumen via a transintestinal rather than the hepatobiliary pathway.

In the bile duct ligation experiment, the amount of 4F recovered in the SI rinse in both experimental and control animals was many-fold lower than observed previously (compare Figs. 2B and 3A). During the bile duct ligation experiment, the animals were under constant isoflurane anesthesia, which has been shown to significantly reduce gastrointestinal motility in rats (69). It is thus possible that the anesthesia itself depressed baseline intestinal clearance of 4F in this experiment. Moreover, the bile duct ligation model excludes from the SI lumen biliary delivery of cholesterol and, importantly, bile salts, which are important modulators of the transintestinal efflux of cholesterol (70). We thus sought to confirm that 4F can indeed transport from intestinal tissue into the SI lumen by intravenously administering 4F in vivo before studying its clearance from duodenal explants ex vivo within a Ussing chamber, an ex vivo physiological system for detecting and quantifying the transport of ions and drugs across epithelial tissues (61). We intravenously administered 800 μg D-4F (~25–30 mg/kg) into C57BL/6J mice (n = 7). We had previously observed that the concentration of 4F associated with the duodenum achieved its maximum around 30 min postinjection (see Fig. 1B). Thus, after 30 min we euthanized the animals and mounted duodenal explants within Ussing chambers that contained bile salt-containing micelles in their mucosal media and lipoproteins in their serosal media (see Materials and Methods for micelle and lipoprotein compositions). We then sampled the mucosal media from 0 to 90 min and determined the levels of intact D-4F released from the explants by LC/MS/MS. We observed a steady increase in D-4F transported from duodenal epithelium into the mucosal-side media across 90 min, with most of the transport occurring within the first 30 min, and with an average of 45 ng of D-4F released from the 0.1 cm^2 of exposed epithelium by 90 min (Fig. 3B).
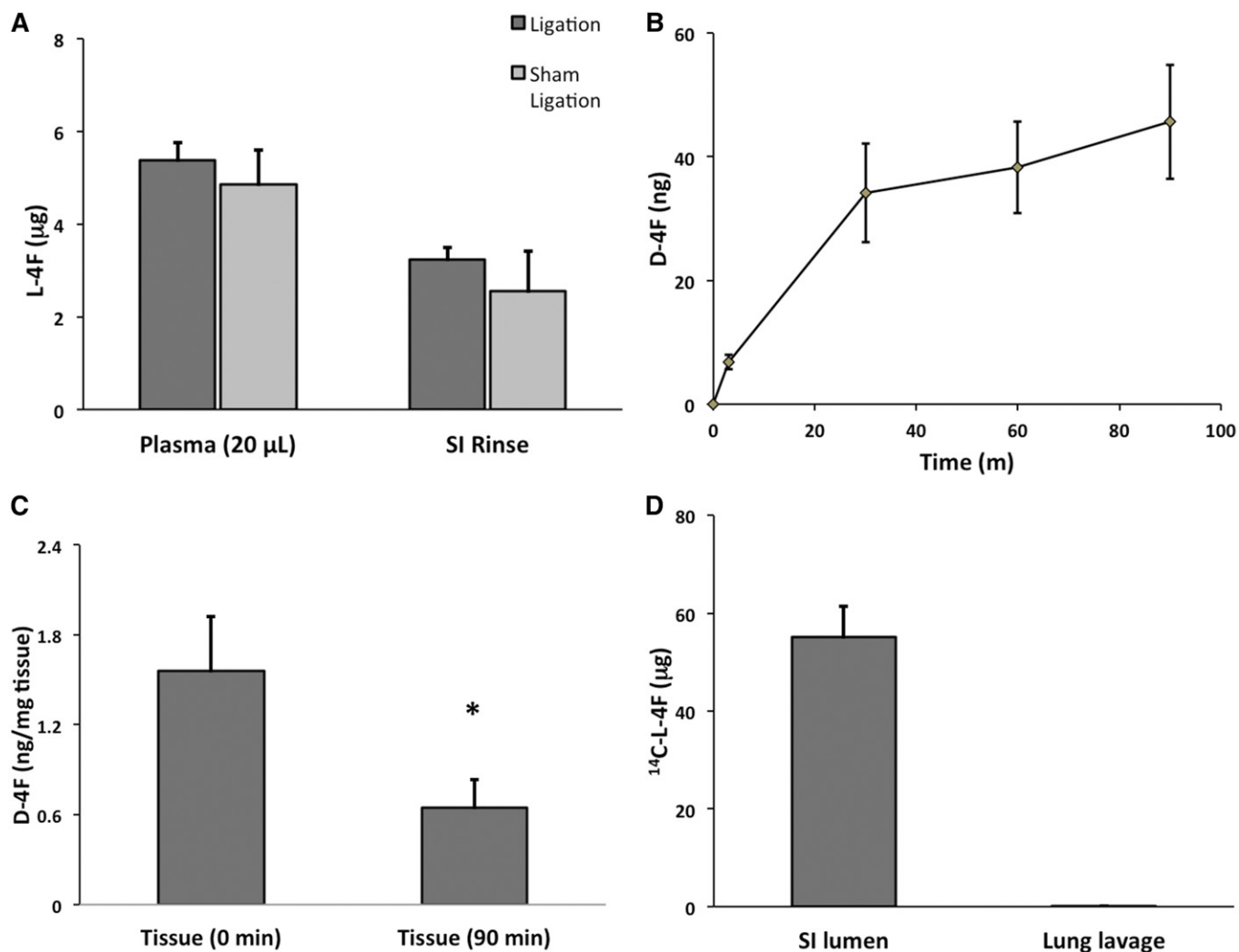
Fig. 3. L-4F enters the intestinal lumen by directly and selectively crossing the intestinal epithelium. A: L-4F (25 mg/kg) was introduced via tail vein into C57BL/6J mice, whose bile ducts had either been ligated or sham ligated (n = 4). Intact L-4F present in the plasma and SI PBS rinse after 1 h was quantified by LC/MS/MS. B, C: C57BL/6J mice (n = 7) were injected with 800 µg (∼25–30 mg/kg) of D-4F via tail vein. After 30 min, the mice were euthanized, and duodenal explants were mounted in Ussing chambers. Serosal side media contained LDL and HDL, while mucosal side media included micelles. Mucosal side media was sampled at 3, 30, 60, and 90 min; and the amount of D-4F present was determined by LC/MS/MS. Peptide was observed released from the tissue into the mucosal side media across 90 min (B). Levels of D-4F were also quantified in these duodenal explants together with matched controls from the same mice. The controls were not mounted in the Ussing chamber and provide the baseline or time zero concentration of D-4F in the tissue (C). Ussing chamber mounted tissue after 90 min had significantly less D-4F than controls (* $P < 0.05$). D: In order to determine whether L-4F selectively crosses intestinal epithelium, the level of L-4F present in lung alveolar space was determined via lung lavage following two individual 25 mg/kg injections of ^{14}C-L-4F at 1 and 3 h prior to being euthanized (n = 6). No L-4F was present in the lung lavage, in contrast with SI PBS rinse. The dpm were converted to µg L-4F. Error is reported as SEM.

Extrapolating from the amount of 4F released from 0.1 cm^2 explants to the ∼7 cm^2 of the entire duodenum (71), ∼3 µg of transportable 4F was present in the duodenal tissue at 30 min postinjection. We also observed that the concentration of D-4F in these explants significantly decreased by ∼60% after the 90 min ex vivo run ($P < 0.05$), compared with paired control tissues that had not been mounted in the Ussing chambers (Fig. 3C). While we chose to use D-4F in this experiment in order to sidestep the possibility of proteolysis of L-4F within the mucosal media over 90 min, we observed comparable transport when we repeated the experiment using L-4F (data not shown).

The experiments represented in Fig. 3A–C establish not only that transintestinal secretory transport of 4F is possible

(Fig. 3B, C), but also that at least under some conditions, all circulating 4F that ends up present in the intestinal lumen arrives via a transintestinal rather than hepatobiliary pathway (Fig. 3A). We last sought to determine whether 4F selectively targets intestinal epithelium or whether 4F crosses any large epithelial barrier. We thus again intravenously administered 25 mg/kg ^{14}C-L-4F to C57BL/6J mice (n = 6). After 1 h, we euthanized the animals and lavaged the lungs with PBS in order to assess transalveolar secretory transport via scintillation counting. We also determined radioactivity present in the SI rinse. In contrast to the SI rinse, we observed no label present in the lung lavage (Fig. 3D) demonstrating comparative intestinal epithelium specificity.

## Intestinal transport of circulating 4F is modulated by TICE

We began our investigation into the mechanism of the transintestinal secretory transport of 4F by first intravenously administering low (25 mg/kg) and high (100 mg/kg) doses of L-4F to C57BL/6J mice (n = 4 and 6, respectively) and then after 1 h determining the levels of intact peptide in the SI PBS rinse by LC/MS/MS. We observed no significant difference as regards transport of intact peptide into the lumen ($P = 0.4$) (**Fig. 4A**). This result indicated that some aspect of the secretory transport pathway was saturable at high doses.
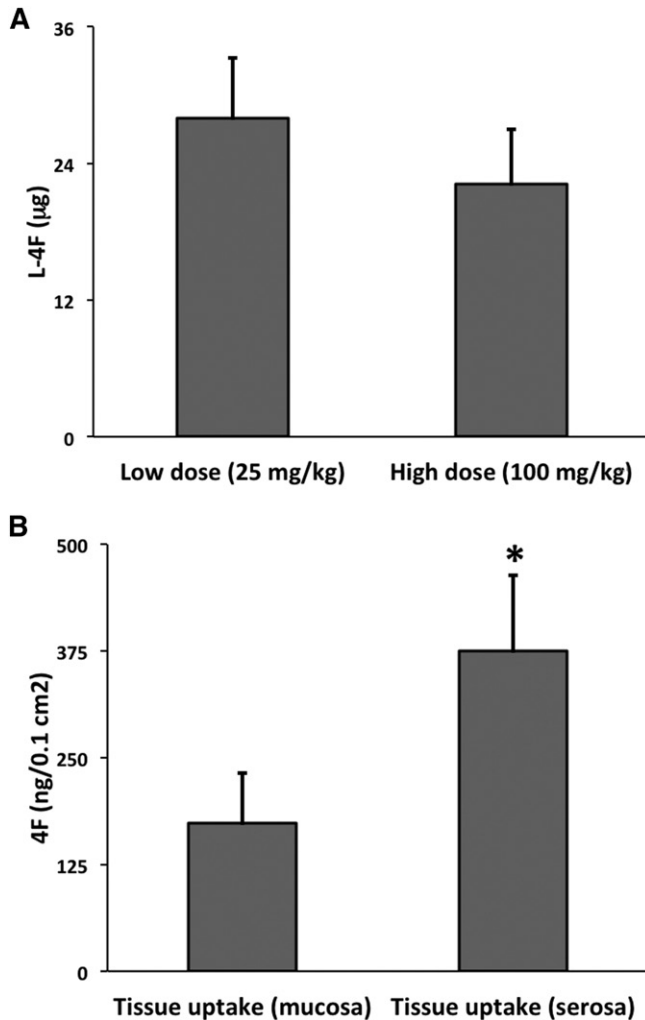
Fig. 4. The process of L-4F secretory transport is saturable, while in turn luminal-side L-4F can itself be taken up into the SI tissue. A: Low-does (25 mg/kg) and high-dose (100 mg/kg) L-4F was introduced via tail vein into C57BL/6J mice (n = 4 and 6, respectively). After 1 h, the level of L-4F in the SI lumen rinse was determined by LC/MS/MS. No significant difference was found between the two doses ($P = 0.4$), indicating that the secretory transport pathway is saturable. B: L-4F or ^{14}C-L-4F + L-4F was added to either the mucosal or serosal media of the Ussing chamber, and uptake by the tissue was determined by LC/MS/MS or scintillation counting respectively (n = 7/group). Duodenal explants took up significantly more 4F from the serosal media than from the mucosal media (* $P < 0.005$). Error is reported as SEM.

We had observed that the concentration of 4F was highest in the proximal small bowel (see Fig. 1C, D). TICE is also greatest in the proximal small bowel (25, 28). We had previously reported that 4F binds with high affinity to lipoproteins including VLDL and HDL (44), as well as to cholesterol alone (50). Lipoproteins including LDL and VLDL (48) and possibly HDL (49) deliver cholesterol from the circulation to the basolateral side of small intestinal enterocytes, and TICE is itself an active and saturable pathway (25). We thus hypothesized that the transintestinal secretory transport of 4F could be modulated by TICE. Consistent with this hypothesis the 90 min uptake of 4F from the serosal side was significantly greater than from the mucosal side of duodenal explants in a Ussing chamber (Fig. 4B).

In order to further test this hypothesis, we required a model that would allow us to manipulate TICE while observing the effect on the secretory transport of 4F. A diet high in fat and cholesterol has been reported to increase TICE by 50–100% in WT mice (70). This effect of WD on TICE is enhanced several fold in NPC1L1$^{-LiverTg112}$ mice (Tg112 mice), which secrete little to no biliary cholesterol but whose levels of both cholesterol absorption and fecal neutral sterols are comparable to WT regardless of diet (32). We thus obtained two male mice hemizygous for the NPC1L1 transgene. We bred these mice with WT C57BL/6J females: genotyping demonstrated the presence of the human NPC1L1 transgene (677 bp) together with a VLDL-specific positive control (320 bp) in half of the offspring, as predicted (supplementary Fig. 2). For further validation, we measured fecal neutral sterol levels by GC/MS (56) in the Tg112 offspring and found no difference compared with the levels in WT mice, consistent with prior reports (**Fig. 5A**) (31, 32). We next fed both male and female Tg112 mice and littermate controls (n = 4 mice/gender/group) a WD or chow for 6 weeks, after which we intravenously administered 675 μg per mouse (∼25 mg/kg) ^{14}C-L-4F to all mice. After 1 h, the mice were euthanized, and label was determined in the SI rinse by scintillation counting. Both male and female mice had significantly more 4F transport into the SI lumen on WD compared with control ($P = 0.007$ and 0.005, respectively). Interestingly, while male and female mice showed no significant difference with respect to 4F secretory transport when on chow ($P = 0.2$), male mice exhibited more such 4F transport than female mice when both were fed WD ($P = 0.008$) (Fig. 5B). As all mice in the current experiment had been dosed at 675 μg ^{14}C-L-4F/mouse (rather than 25 mg/kg as before), this sex difference as regards 4F transport was not due to the heavier male mice receiving more total peptide. Fortuitously, this unexpected difference also allowed us to use fecal neutral sterol levels as a marker for TICE in these two groups, in order to confirm that enhanced 4F transport correlates with enhanced TICE in this model. If one were comparing chow- versus WD-fed animals alone, the relation between TICE and fecal neutral sterol levels would be confounded by the difference in the cholesterol content of the diets themselves. Thus, the fact that WD-fed animals had higher levels of fecal neutral sterols would not
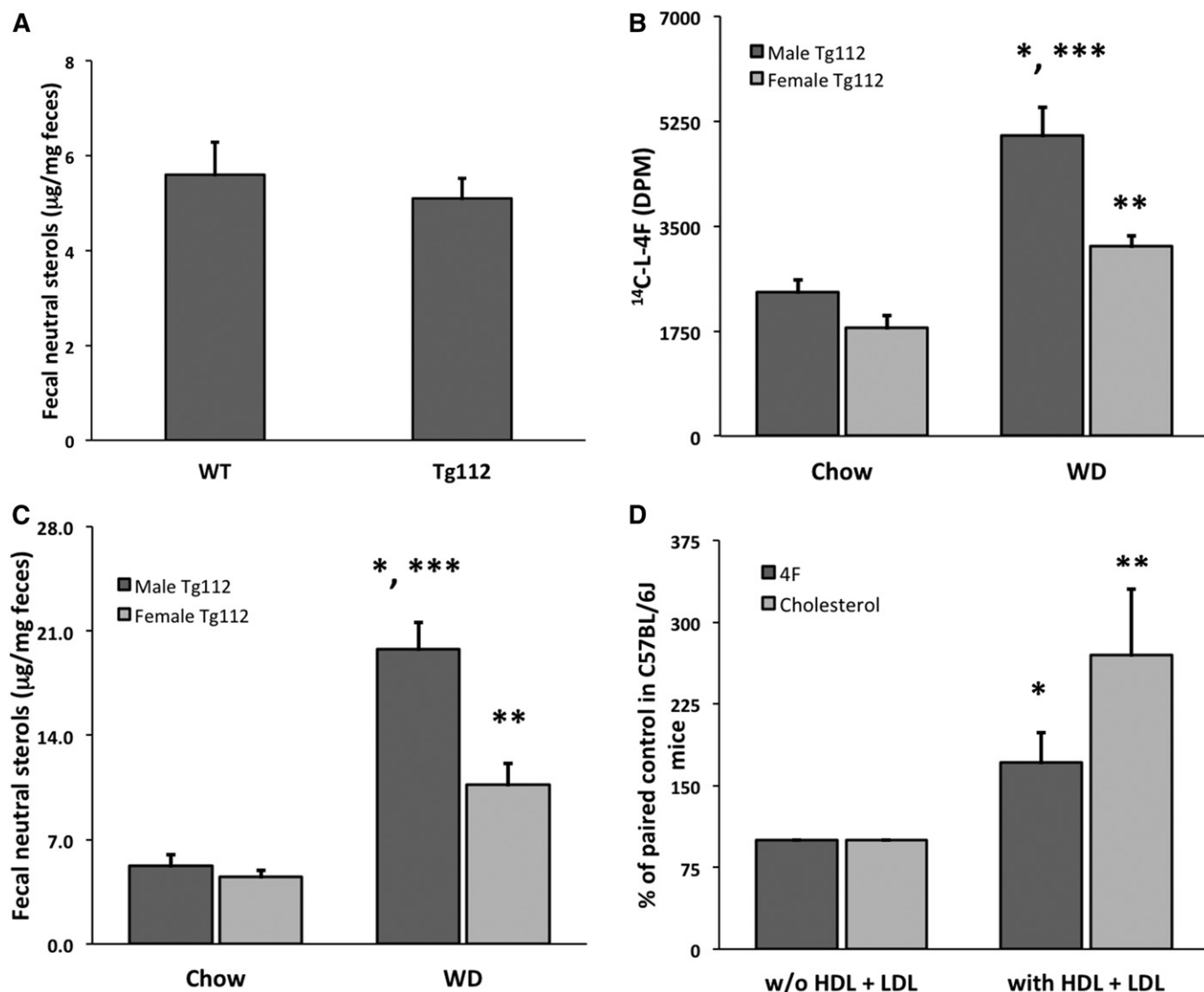
Fig. 5. The secretory transport of 4F is modulated by TICE. A: Levels of neutral sterols in the feces from Tg112 and littermate control mice fed a chow diet (n = 8/group) were compared by GC/MS. B: WD has been shown to upregulate TICE in Tg112 mice. Male and female Tg112 mice were fed chow or WD for 6 weeks (n = 4 mice/gender/group), injected with 675 μg per mouse of ^{14}C-L-4F (∼25 mg/kg) via the tail veins, and the radioactivity in the lumen washes was determined after 1 h. WD significantly upregulated 4F transport in both male (* $P = 0.007$) and female mice (** $P = 0.005$). While male and female mice exhibited no significant difference on chow ($P = 0.2$), male mice had significantly higher transport of 4F into the SI lumen than female mice when both were fed a WD (*** $P = 0.008$). C: Total neutral sterols were determined by GC/MS in the feces of the individual mice in B. WD significantly increased neutral sterols in the feces of both male (* $P = 0.001$) and female mice (** $P = 0.02$). While male and female mice exhibited no significant difference on chow, male mice had significantly more neutral sterols in their feces compared with female mice when both were fed a WD (*** $P = 0.01$). D: C57BL/6J mice were injected with 800 μg (∼25–30 mg/kg)/300 μl saline of D-4F via their tail veins (n = 7). After 30 min, the mice were euthanized and duodenal tissue explants were mounted in Ussing chambers. Each mouse contributed paired explants, whose serosal side media both did or did not contain LDL + HDL. Levels of both D-4F and cholesterol in mucosal media were determined by LC/MS/MS and GC/MS, respectively. The presence of serosal side lipoproteins significantly enhanced the transport of both D-4F and cholesterol into the mucosal media (*, ** $P < 0.05$). Error is reported as SEM.

itself tell us that these animals exhibited greater TICE: the difference could be the mere result of the pass-through or incomplete absorption of the cholesterol in the food. Both the male and female mice of our final comparison were on WD, however, thereby removing this particular confounding variable. We thus determined by GC/MS the fecal neutral sterol levels of the individual mice of Fig. 5B. Of interest, male mice on WD had significantly higher levels of neutral sterols in their feces compared with female mice

on WD ($P = 0.01$) (Fig. 5C), independently supporting the conclusion that the levels of 4F secretory transport in this experiment correlated with the levels of TICE.

Nonetheless, WD presumably has many effects on Tg112 mice beyond increasing TICE. Even if we allow that the experiment of Fig. 5B, C establishes a correlation between TICE and 4F secretory transport, it does not thereby establish causation. Recently, TICE has been studied using murine duodenal explants within a Ussing chamber system

(49). We thus turned again to the in vivo/ex vivo model of Fig. 3B, in order to study the effect of TICE on the secretory transport of 4F within a simpler system. First, we established the existence of TICE ex vivo by observing the transport of ^{3}H-cholesterol across duodenal explants from C57BL/6J mice that had been mounted in our Ussing chambers (for an example of baseline TICE within the Ussing chamber system, see the control group of Fig. 7A). Next, we intravenously administered 800 µg D-4F (~25–30 mg/kg) to C57BL/6J mice (n = 7), and after 30 min we euthanized the mice and mounted within Ussing chambers duodenal explants together with matched controls from the same animals. For every matched pair, the serosal media of one explant contained HDL + LDL while the media of the other explant was basic serosal media alone, and the mucosal media for all samples contained micelles (for micelle and lipoprotein compositions, see Materials and Methods). We sampled the mucosal media across 90 min and determined the concentrations of D-4F and cholesterol present in the media at 30 and 60 min (data not shown), as well as at 90 min, by LC/MS/MS and GC/MS, respectively. We observed that the presence of serosal-side lipoprotein significantly enhanced the transport of both D-4F (by 171%) and cholesterol (by 270%) from the experimental explants into the mucosal media compared with the matched controls ($P = 0.044$ and 0.047) (Fig. 5D). This experiment was conducted pair-wise, in order to compensate for the possibility of variable loading of 4F into the duodenum. The data in Fig. 5D are thus expressed as percent change compared with the matched controls. However, total 4F and cholesterol averaged across all groups also increased, from ~80 ng (0.034 nmol) 4F and 110 ng (0.28 nmol) cholesterol to 120 ng (0.052 nmol) 4F and 260 ng (0.67 nmol) cholesterol. Of further note, the secretory transport of 4F over time mirrored that of Fig. 3B: approximately linear through 30 min before tapering off to 90 min.

Our results from the above two separate models (in vivo and ex vivo) suggest that transintestinal secretory transport of 4F can be modulated by TICE. In both models, the degree of TICE correlates with the degree of 4F transport. While it is possible that in either model taken by itself, the initiating cause (WD on the one hand, serosal-side lipoproteins on the other) could independently increase both TICE and 4F transport, the existence of correlations between 4F transport and TICE in two separate models strongly suggests a causal connection between both processes.

Intravenously administered 4F increases macrophage RCT and cholesterol efflux from lipoproteins in Tg112 mice

Transintestinal efflux of cholesterol appears to help drive 4F transport from intestinal epithelium. 4F also binds with high affinity to lipoproteins (44) and to cholesterol (50). These facts suggest a model in which 4F associates with cholesterol as it is taken up and transported apically by enterocytes. What of the converse: does 4F transport itself modulate cholesterol efflux? Oral D-4F can

increase macrophage RCT (72). While 2 week treatment of 45 mg/kg/day oral D-4F only achieves plasma Cmax of ~500 ng/ml, the concentration of D-4F at that dose in intestinal tissue is markedly higher, with ~100 µg present in the SI (5). As shown in Fig. 4D, in duodenal explants not only is 4F taken up from the serosal media, it can be taken up from mucosal media as well. These facts suggest that the mechanism by which oral 4F increases macrophage RCT is at least partially intestinal in nature, perhaps through the upregulation of TICE. As intravenously administered 4F achieves concentrations in the intestine comparable to that achieved by high dose oral D-4F [compare Fig. 1C, D with Table 1 in (5)], we hypothesized not only that intravenously administered 4F could increase macrophage RCT, but that it would do so at least in part by modulating TICE.

Temel et al. (32) investigated macrophage RCT using the Rader protocol (63), and they showed no difference in cholesterol excretion between Tg112 and WT mice. While intestinal cholesterol absorption was unchanged in Tg112 mice compared with controls, biliary sterol secretion was largely inhibited (>90% reduction). Temel et al. (32) concluded that only TICE could account for the fact that cholesterol excretion in Tg112 mice was nonetheless comparable to that in WT mice, and they thus concluded that TICE could modulate macrophage RCT. They supported this latter conclusion by repeating the macrophage RCT experiment in bile-diverted versus surgical control mice and again found no difference in luminal cholesterol excretion, further establishing that macrophage RCT can indeed follow the TICE pathway (32). However, others have called this conclusion into question. Of note, Njistad et al. (73) assessed macrophage RCT using $Abcb4^{-/-}$ mice as well as in a bile duct ligation model, and they observed that in the absence of biliary cholesterol secretion macrophage RCT was mostly ablated.

Because of this controversy, we first repeated the macrophage RCT experiment of Temel et al. (32) in Tg112 vs. WT mice, with modification. In particular, we applied their protocol for studying ^{3}H-cholesterol efflux in the biliary diversion model to the study of TICE in Tg112 mice (63). Thus, we loaded J774 macrophages with acetylated LDL and ^{3}H-cholesterol and at time t = 0 h administered the macrophages by intraperitoneal injection to both Tg112 and WT mice. At t = 8 h, the mice were euthanized, the luminal contents of the entire SI were collected with a PBS rinse, and a chloroform/methanol extraction was performed. Radioactivity in the chloroform phase was determined, as a measure of ^{3}H-cholesterol, while radioactivity in the aqueous phase was also determined, as a measure of ^{3}H-bile acids (**Fig. 6A**). When Temel et al. studied macrophage RCT in Tg112 mice, they measured ^{3}H-cholesterol in the feces, and they observed no difference in cholesterol efflux between Tg112 and WT mice. Consistent with this observation, we saw no difference in ^{3}H-cholesterol efflux into the lumens of Tg112 and WT mice.

We next asked whether intravenous administration of L-4F could increase macrophage RCT in both Tg112 and WT mice. The timeline for this experiment was as follows:
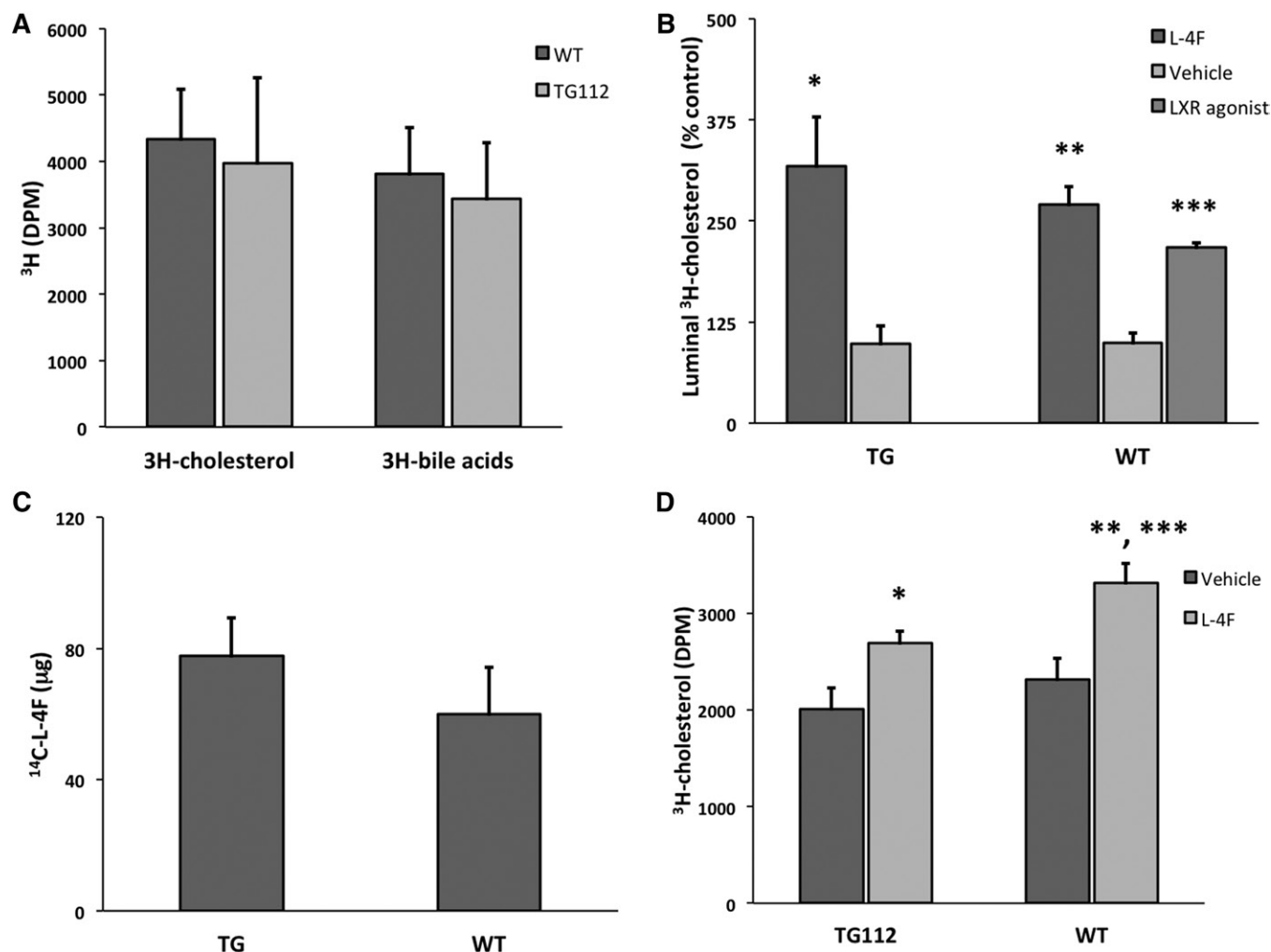
Fig. 6. Circulating L-4F increases RCT from macrophages and cholesterol efflux from lipoproteins in Tg112 mice. A: Macrophage RCT was determined in Tg112 mice compared with littermate controls (WT). J774 cells were grown in culture and loaded with acetylated LDL that had been labeled with ^{3}H-cholesterol. Loaded macrophages were injected intraperitoneally ($\sim$2 × 10^6 cells and 1 μCi per mouse) into both WT and Tg112 mice (n = 4/group). After 8 h, the mice were euthanized, and lumen rinse was collected. Following chloroform/methanol extraction of the rinse, label was determined by scintillation counting in both the chloroform fraction (^{3}H-cholesterol) and the methanol/water fraction (^{3}H-bile acids). B: We determined the effect of intravenously administered L-4F on macrophage RCT. We proceeded as in A, except that the mice were intravenously administered either 25 mg/kg ^{14}C-L-4F or vehicle at both t = 4 h and t = 7 h (n = 5/group). As positive control, 3 WT animals had received 1 week pretreatment with the LXR agonist T0901317; these were otherwise treated as vehicle controls. L-4F significantly increased RCT into the intestinal lumen for both Tg112 (* P = 0.01) and WT (** P = 0.001) mice. LXR agonist treatment likewise increased RCT (*** P = 0.03). Data are expressed as percent of the corresponding vehicle controls. C: ^{14}C label was determined in the luminal PBS rinse of both the Tg112 and WT mice from B, and dpm were converted to μg ^{14}C-L-4F. D: In order to investigate the mechanism by which 4F modulates RCT, we repeated the basic experiments of A and B except that we used HDL and LDL rather than macrophages as the cholesterol source. Human LDL and HDL were prelabeled with ^{3}H-cholesterol. The lipoproteins were then premixed with either ^{14}C-L-4F or vehicle, and 100 μg HDL cholesterol + 100 μg LDL-C + 25 mg/kg ^{14}C-L-4F (or vehicle) was injected via tail vein into both Tg112 and WT mice (n = 7 mice/group). At t = 3 h, the mice were given a second injection of either 25 mg/kg ^{14}C-L-4F or vehicle. At t = 4 h the mice were euthanized, and radioactivity was determined as before. ^{14}C-L-4F significantly increased cholesterol efflux into the SI lumen in both Tg112 (* P = 0.004) and WT (** P = 0.001) mice. The effect in Tg112 mice strongly suggests that L-4F can upregulate cholesterol efflux via the TICE pathway. In this experiment, however, L-4F also significantly increased cholesterol efflux in WT mice compared with Tg112 mice (*** P = 0.04), suggesting that L-4F also affects cholesterol efflux through the hepatobiliary pathway in this context. Error is reported as SEM.

at t = 0 h, we administered by intraperitoneal injection ^{3}H-cholesterol-loaded J774 macrophages to both Tg112 and littermate control mice; at t = 4 h, we intravenously administered 25 mg/kg ^{14}C-L-4F or saline vehicle (n = 5 mice/group = 20 total mice); at t = 7 h, we intravenously administered a second equal dose of ^{14}C-L-4F or saline vehicle; at t = 8 h, we euthanized the animals and analyzed the luminal rinse. Of note, we observed that intravenously administered 4F significantly increased ^{3}H-cholesterol efflux into the lumen in both Tg112 and WT mice (Fig. 6B). We further detected comparable levels of ^{14}C-L-4F in the lumens of both Tg112 and WT mice (Fig. 6C).

The result of Fig. 6B establishes that intravenously administered 4F can increase macrophage RCT in Tg112

mice, but it does not reveal whether 4F increases cholesterol efflux as such. Indeed, we observed, consistent with the observations of Xie et al. (72), that 4F can dose-dependently increase cholesterol efflux from J774 foam cells in vitro (supplementary Fig. 3). Thus, one possibility is that 4F increased labeled cholesterol efflux from the J774 cells in vivo leading to higher levels of plasma labeled cholesterol, while the increase of labeled cholesterol in the SI was due solely to this effect without any direct effect of 4F on TICE. In order to address this possibility, we repeated the experiment of Fig. 6B, except that we eliminated macrophages and directly administered HDL and LDL that had been loaded with ^{3}H-cholesterol (Fig. 6D).

In choosing to introduce the labeled cholesterol together with HDL and LDL, we sought a generous system that would give us our best chance of independently observing an effect of 4F on cholesterol efflux into the SI lumen. While there exists evidence in the literature that HDL can play the role of lipoprotein carrier for TICE (49), there are competing studies that have indicated that apoB-containing lipoproteins are the carriers (48). Because of this uncertainty, we combined both HDL and LDL together when we introduced labeled cholesterol directly into the circulation in the experiment of Fig. 6D.

In this experiment, we once again observed that intravenously administered 4F significantly increased luminal ^{3}H-cholesterol efflux in both Tg112 and WT mice, suggesting that any effect 4F might have had on the efflux of cholesterol from J774 macrophages was not the sole cause of the effect of 4F on macrophage RCT. Rather, intravenously administered 4F directly increases cholesterol efflux from the circulation into the SI. Given the nature of cholesterol excretion in Tg112 mice, this result strongly suggests that intravenously administered 4F can increase TICE. Of note, however, the effect of 4F on cholesterol efflux was significantly greater in WT mice compared with Tg112 mice. While we had not observed this difference in the experiment represented in Fig. 6B, this result suggests that in WT mice there remains a hepatobiliary component to the effect of 4F on luminal cholesterol efflux. This possibility is consistent with the results represented in Fig. 2A, in which we observed the presence of ^{14}C label within the contents of the gall bladder.

4F increases TICE through duodenal explants and can act as a cholesterol acceptor with respect to cholesterol efflux from enterocytes

While the experiment of Fig. 6D establishes that 4F modulates luminal cholesterol efflux in both Tg112 and WT mice in a macrophage-independent manner and strongly suggests that 4F can modulate TICE, it does not fully prove the latter. Cholesterol secretion into bile is severely diminished in Tg112 mice, but it is not entirely abrogated (32). It thus remains possible that 4F increases luminal cholesterol efflux in Tg112 mice solely by modulating this residual biliary cholesterol secretion. We thus turned once again to the Ussing chamber in order to ask the question whether 4F can in fact increase TICE. As in the experiment represented in Fig. 5D, we first loaded 4F

into intestinal tissue in vivo by intravenously administering 800 μg D-4F (∼25–30 mg/kg) to C57BL/6J mice. After 30 min, we euthanized the animals and mounted duodenal explants into Ussing chambers, together with explants from animals that had not been administered 4F. The serosal media contained HDL and LDL that had been loaded with ^{3}H-cholesterol, and we determined radioactivity in the mucosal media at 90 min (**Fig. 7A**). We observed that the presence of 4F within the explants significantly increased the transintestinal efflux of labeled cholesterol while also significantly increasing the loading of ^{3}H-cholesterol into the duodenal explants.

The results reported in Fig. 7A suggest two basic mechanisms. First, 4F could act within the tissue, where it could draw more serosal-side cholesterol into the tissue itself or where it could act as an internal chaperone with respect to cholesterol efflux. Second, 4F within the tissue is transported into the mucosal media (see Fig. 3B), where it would be well positioned to act as a cholesterol acceptor with respect to TICE. In order to partially test this second possibility, we stripped enterocytes from C57BL/6J mice and loaded them with ^{3}H-cholesterol. We observed that 4F dose-dependently increased cholesterol efflux from these loaded cells (Fig. 7B). While this result is consistent with 4F acting as a cholesterol acceptor in the experiment of Fig. 7A, the primary enterocytes of Fig. 7B were nonpolarized. This experiment thus failed to determine whether 4F could increase cholesterol efflux from apical-side rather than basolateral-side transporters. Because of this limitation, we made use of the polarized nature of duodenal explants within our Ussing chambers to investigate the effect of mucosal-side 4F on TICE proper. We mounted within Ussing chambers duodenal explants together with matched controls from the same animals. As in Fig. 7A, we added ^{3}H-cholesterol loaded LDL + HDL to the serosal media. For each pair of explants, the mucosal media contained either micelles together with D-4F or micelles together with vehicle alone. We observed that mucosal-side 4F significantly increased ^{3}H-cholesterol loading into the explants, while also significantly increasing the efflux of labeled cholesterol into the mucosal media itself (Fig. 7C). Of note, when we attempted the experiment of Fig. 7C in the absence of micelles, we observed neither a stable baseline TICE nor a consistent effect of 4F (data not shown). This result is in contrast to that of Fig. 7B, in which 4F promoted cholesterol efflux from primary enterocytes even in the absence of micelles. These observations suggest that micelles are an important necessary condition on TICE ex vivo, and in this they are consistent with the necessary role of micelles for in vivo TICE that has been reported in the literature (70).

DISCUSSION

We have here observed that circulating 4F selectively targets the SI (Fig. 1), where it is largely transported intact into the SI lumen (Fig. 2) in a transintestinal process (Fig. 3) that is at least partially mediated by TICE (Fig. 5). In
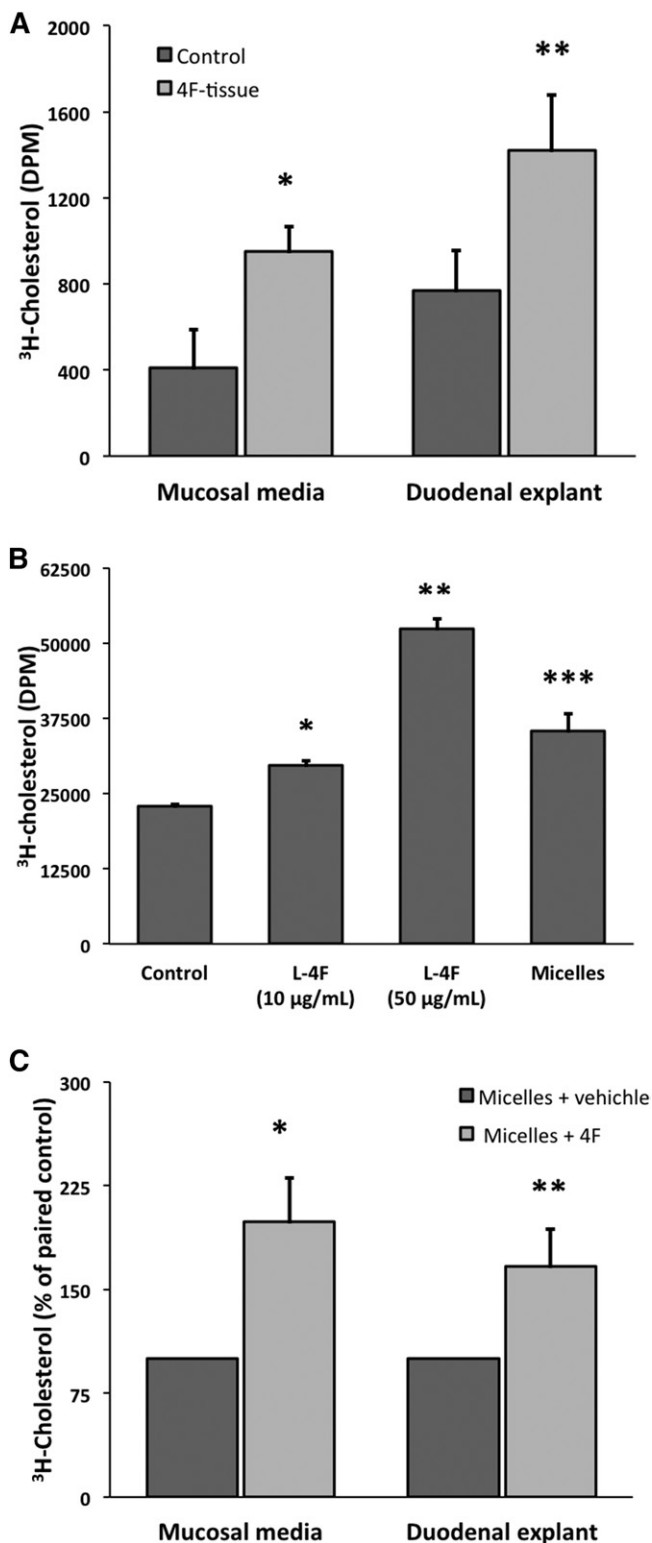
Fig. 7. 4F increases TICE through duodenal explants and can act as a cholesterol acceptor with respect to cholesterol efflux from enterocytes. A: 800 μg D-4F (∼25–30 mg/kg)/300 μl saline or vehicle was injected into the tail veins of C57BL/6J mice (n = 5). After 30 min, the mice were euthanized and duodenal explants from the mice injected with 4F (4F-tissue) and vehicle (control) were mounted in Ussing chambers. After 30 min in vivo, the explants from 4F-injected mice had been preloaded with 4F (see Fig. 3B). The mucosal media for both groups contained fresh micelles, while all serosal media contained a fresh-mixed combination of human HDL and LDL that had been preloaded with 1 μCi/well of ^{3}H-cholesterol. The mucosal media were sampled through 90 min, and total ^{3}H-cholesterol effluxed into the mucosal media during that time was determined by scintillation counting. At the end of the experiment, ^{3}H-cholesterol level in the tissues was also determined. Preloading the tissue with 4F significantly increased the amount of cholesterol label in both the mucosal media and the duodenal explants (*, ** $P < 0.05$). B: Primary enterocytes were stripped from the SI using EDTA and loaded with ^{3}H-cholesterol for 30 min under constant aeration. The cells were washed and media changed, and L-4F was added to the cell suspensions. Micelles alone were also added as a positive control (n = 3/group). L-4F dose dependently increased ^{3}H-cholesterol efflux from enterocytes (control vs. 10 μg/ml, * $P = 0.001$; 10 μg/ml vs. 50 μg/ml, ** $P = 0.0002$; control vs. micelles, *** $P = 0.01$). C: Duodenal explants from C57BL/6J mice were mounted in Ussing chambers. Each mouse contributed two contiguous explants, whose serosal-side media contained ^{3}H-cholesterol loaded lipoproteins (as above). For each pair, either 50 μg/ml D-4F or vehicle was added to mucosal-side media that contained micelles. Mucosal-side 4F significantly increased cholesterol loading into the explants (** $P = 0.044$) as well as cholesterol efflux into mucosal media themselves (* $P = 0.047$) compared with the paired controls. Error is reported as SEM.

turn, the transintestinal secretory transport of 4F can itself modulate TICE (Figs. 6, 7), at least in part by acting as a cholesterol acceptor within the SI lumen (Fig. 7). 4F has been shown to be effective as a treatment for atherosclerosis and other inflammatory conditions (38, 39, 74). Although 4F has been hypothesized to increase the clearance of proinflammatory and oxidized lipid species from the circulation (44), a mechanism common to 4F's efficacy in various inflammatory disease models is not yet known. Our findings may thus help illuminate a mechanism of action of 4F. Independently, we have here identified a novel modulator of TICE, a finding of potential importance regarding the basic biology and pharmacological manipulation of this cholesterol excretion pathway.

In support of our prior hypothesis that the intestine is the site of action of 4F, we have shown here that circulating 4F selectively targets the proximal small bowel (Fig. 1). Moreover, we have characterized the basic mechanism by which circulating 4F targets the SI.

First, while we had previously speculated that circulating 4F might reach the SI solely through the hepatobiliary pathway (46), we have now established that 4F is transintestinally transported into the SI lumen (Figs. 2, 3). While these findings do not preclude 4F reaching the SI lumen through the bile, the kinetics of 4F within the bile appear out of phase with the kinetics of 4F transport into the SI lumen (Fig. 2A). Moreover, under anesthesia at least, all 4F transport into the SI lumen is transintestinal (Fig. 3A), and the amount of 4F transport from duodenal explants ex vivo is consistent with the transintestinal pathway being predominant (Fig. 3B).

Second, we have established that TICE can modulate the transintestinal transport of 4F (Fig. 5). WD enhances TICE in Tg112 mice (32). Correlative with this effect, WD increased the transintestinal transport of 4F (Fig. 5B, C). We also observed that the secretory transport of 4F that

had been preloaded into duodenal explants can itself be enhanced by serosal-side lipoproteins and their attendant TICE (Fig. 5D). This result together with those of Fig. 5B, C, ex vivo and in vivo models of enhanced TICE exhibiting enhanced transintestinal 4F transport, strongly support the conclusion that 4F transport can be modulated by TICE. Because 4F appears to associate with lipoproteins in the circulation (44), and because TICE involves the uptake of circulating lipoproteins by the basolateral membranes of enterocytes (24–28), it is possible that some of the increase in 4F that we observed in Tg112 mice on WD is the result of increased targeting of circulating 4F to enterocytes (Fig. 5B, C). However, we also observed that the transport of 4F that had been preloaded into duodenal explants can itself be enhanced by serosal-side lipoproteins and their attendant TICE (Fig. 5D). The results of Fig. 5D indicate that at least part of the mechanism by which TICE can enhance 4F transport is intraepithelial in nature. The saturability of the 4F transport pathway (Fig. 4A) further suggests that the mechanism is transcellular. It may thus seem reasonable to hypothesize that 4F, having been carried through the circulation associated with lipoproteins and having loaded into enterocytes basolaterally, coeffluxes with intracellular cholesterol through transporters on the apical membranes of enterocytes. This hypothesis is strengthened by the fact that 4F also binds cholesterol with high affinity (50). As against this model, however, it is worth noting that while we ourselves have shown that 4F associates with lipoproteins in vivo, there exist some reports in the literature that 4F does not bind to the lipoprotein fraction of the plasma in vivo (75). More importantly, the stoichiometry involved weighs against a simple coefflux model. In the experiment associated with Fig. 5D, $\sim$0.02 nmol peptide together with $\sim$0.3 nmol cholesterol were transported into the mucosal-side media, for a molar ratio of about 1:15. Given the size and conformation of 4F, it is unlikely that one peptide molecule associates with 15 cholesterol molecules during any single coefflux event. However, it remains possible that peptide could coefflux with cholesterol at a higher molar ratio, only for peptide then present at the apical boundary of enterocytes to further enhance the efflux of cholesterol itself, perhaps through additional transporters (see Fig. 7B, C).

Lipoproteins and cholesterol can be taken up by enterocytes through LDLR as well as possibly scavenger receptor class B type I located on their basolateral membranes, and intracellular cholesterol is effluxed through the apical membranes via abcg5/g8 as well as abcb1a/b (49). Abcb1, also known as P-glycoprotein 1 or multidrug resistance protein 1, is a member of the ATP-binding cassette transporters subfamily B. Abcb1 is an ATP-dependent drug efflux pump for xenobiotic compounds with broad substrate specificity, but it can also act as a cholesterol floppase (76) and has been shown to contribute to TICE (49). Abcb1 is thus a good candidate for the apical transporter of 4F, perhaps explaining why there exists baseline 4F transport from duodenal explants even in the absence of TICE, but why serosal-side lipoproteins nonetheless significantly

increase 4F transport (Fig. 5D). We are continuing to investigate the precise molecular mechanism by which 4F is taken up from the circulation and transported into the intestinal lumen by the proximal SI.

The 4F secretory transport pathway hypothesized above could account for the manner in which SQ-administered 4F lowers levels of oxidized lipids including HETEs and HODEs in intestinal tissue and enterocytes (5, 77). 4F binds these oxidized lipids with high affinity (50). If circulating lipoproteins target 4F for basolateral uptake by enterocytes, and if 4F is subsequently cleared apically through abcb1a/b, for example, 4F could carry with it any intracellular lipid species it binds with high affinity. This pathway could also account for the manner in which 4F lowers levels of oxidized lipids in plasma (78) and lipoproteins (44). Finally, orally administered 4F achieves concentrations in intestinal tissue comparable to SQ-administered 4F for a given dose. We have shown here that mucosal-side 4F can be taken up by duodenal explants (Fig. 4B). If 4F taken up from the SI lumen is itself transported back into the lumen as above, this same transport pathway could also account for the manner in which oral 4F lowers levels of oxidized lipids in enterocytes (5). We must continue to investigate, however, whether the reduction of oxidized lipids in the SI is a direct consequence of 4F transport as hypothesized here: whether it is the result of the direct clearance of the oxidized species or whether it is rather the result of, for example, a clearance of substrates like arachidonic acid (5) or an effect upon enzymes including phospholipase A_2 and 12/15 lipoxygenase.

Through the use of the TG112 mouse model (Fig. 6) and our ex vivo Ussing chamber system (Fig. 7), we have established that 4F can modulate the TICE pathway. These findings are of potential importance as regards the mechanism of 4F. While we had previously shown that 4F can increase macrophage RCT in vivo (79), the precise mechanism behind this effect was unknown. The results of Fig. 6B, together with those from Figs. 6D and 7, indicate that 4F can affect macrophage RCT at least in part by modulating TICE. This observation raises the possibility that the common understanding of the antiatherogenic mechanism of 4F may be incomplete. 4F can bind oxidized lipids with much higher affinity than apoAI (50), while its capacity to stimulate cholesterol efflux from macrophages is lower than apoAI on a per molar basis (80, 81). Facts like these have led some to argue that the cholesterol efflux capacity of 4F is of secondary importance at best compared with its antioxidative capacity, as regards its effects on atherosclerosis (82). However, if 4F affects cholesterol efflux and macrophage RCT in vivo at the level of TICE rather than at the level of cholesterol efflux from macrophages themselves, as is suggested by results reported in Fig. 6B, D, then arguments against the importance of cholesterol efflux within the mechanism of 4F based on in vitro studies of cholesterol efflux from macrophages may be misplaced. It is an open question in the literature whether increasing TICE alone can protect against atherosclerosis. Likewise, while our results strongly suggest that 4F can increase macrophage RCT (Fig. 6B) and cholesterol efflux

from the circulation itself (Fig. 6D) in a TICE-dependent manner, we do not here directly link these phenomena to the antiatherogenic effects of 4F. However, our present findings do at least suggest that the effects of 4F on cholesterol excretion and TICE deserve a second look. We are continuing to investigate whether the modulation of TICE by 4F plays an important role in the antiatherogenic mechanism of this peptide.

Our in vivo studies involving the effects of 4F on macrophage RCT and cholesterol efflux from the circulation involved the use of the Tg112 mouse model. While investigating macrophage RCT, Temel et al. showed that sterol secretion was undiminished compared with controls in both Tg112 as well as a biliary diversion model. They concluded that macrophage RCT could proceed via the TICE pathway and not just the hepatobiliary pathway (32). However, in addition to the work of Nijstad et al. (73), Xie et al. showed that macrophage RCT was reduced in Tg112 mice that had been crossed to NPC1L1 knock-out mice (83). Our results here support Temel et al. as regards cholesterol excretion in Tg112 mice during macrophage RCT. Consistent with Temel et al., we observed no difference in the luminal efflux of labeled bile acids and cholesterol in Tg112 mice versus controls with respect to macrophage RCT (Fig. 6A). Given that biliary sterol secretion is severely compromised in Tg112 mice (31, 32), and given that cholesterol absorption does not differ between Tg112 and WT mice (32), our observation that both Tg112 and WT mice exhibited comparable levels of luminal cholesterol excretion in the macrophage RCT experiment of Fig. 6A suggests that most of the cholesterol label that accumulated in the SI lumen in Tg112 mice was a function of TICE.

Our investigation into the effects of 4F on cholesterol efflux took the form of an increasingly narrow or circumscribed investigation into mechanism. We first established that 4F could increase macrophage RCT in Tg112 mice (Fig. 6B). Next, we ruled out the possibility that this first observation was solely the result of 4F enhancing cholesterol efflux from macrophages by observing that 4F could increase cholesterol efflux directly from the circulation of Tg112 mice (Fig. 6D). Finally, we zoomed into the intraduodenal effects of 4F within our Ussing chamber system, and we observed that even here 4F could enhance TICE (Fig. 7A). We then explained this final effect in terms of the role of 4F as cholesterol acceptor on the apical side of enterocytes (Fig. 7B, C). However, these experiments leave open at least two questions.

First, while 4F increased cholesterol efflux into the SI lumen both from foam cells (Fig. 6B) and from circulating lipoproteins (Fig. 6D), suggesting that the mechanism behind the results reported in Fig. 6B contains the mechanism behind the results reported in Fig. 6D, it is nonetheless possible that these overlapping mechanisms may differ in at least two respects. The labeled free cholesterol (FC) from foam cells (Fig. 6B) most likely enters the circulation associated with HDL, where it can be readily converted to labeled cholesteryl esters (CEs) by the activity of LCAT (84). Thus, some good portion of the label from foam cells (Fig. 6B) will be within HDL-associated CEs. By contrast, while the labeled lipoproteins (Fig. 6D) contain HDL, they also contain LDL. And while LCAT is also associated with LDL, the degree of esterification of FC to CE is lower in LDL compared with HDL (84). Thus, the labeled cholesterol present in the circulation in the experiment of Fig. 6D compared to the experiment of Fig. 6B may differ in two respects: initial distribution over LDL and not just HDL, and a higher ratio of FC/CE label. As HDL can transfer both FC (85) and CE (86) to LDL in circulation, the distribution of label over lipoprotein classes may not be different over time between the two routes (Fig. 6B, D). However, while little is known about the differing roles of FC and CE in TICE, it remains possible that 4F may act on the two routes of cholesterol efflux (Fig. 6B, D) in slightly different ways.

Second, while the results reported in Fig. 7B, C strongly suggest that 4F can increase TICE by acting as an apical-side cholesterol acceptor, they do not further elucidate the mechanism involved. For one, these experiments do not identify on which transporters 4F may be acting. Second, they fail to tease apart the role that micelles appear to play in this phenomenon. As mentioned previously, when we conducted the experiments reported in Fig. 7C without micelles, we observed neither consistent baseline TICE nor consistent effects of 4F (data not shown). These observations were in contrast with the experiments shown in Fig. 7B, in which 4F induced cholesterol efflux from primary enterocytes even in the absence of micelles. These results suggest that micelles are an important necessary condition on TICE within an ex vivo system, and as such they are in keeping with prior studies on TICE that identify micelles as something approaching a necessary condition on TICE both ex vivo (49) and in vivo (70). However, we are continuing to investigate the manner in which micelles and 4F act together to promote TICE.

Of interest, few promising pharmacological modulators of TICE have been identified to date. LXR agonists including the compound T0901317 have been shown to upregulate TICE (29), but LXR agonist treatment is accompanied by significant side effects including increased TG and LDL-C levels (87). Studies involving intestinal-specific activation of LXR have demonstrated enhanced macrophage RCT and atheroprotection (88, 89), but as yet the effects of intestinal-specific LXR activation have not been traced back to TICE. Bile acids and phospholipids in the intestinal lumen have been shown to stimulate the amount of cholesterol secreted via TICE (90, 91). Dietary plant sterols including campesterol and sitosterol may also stimulate TICE (92).

We have here identified a novel pharmacological modulator of TICE. 4F could thus serve as an important investigative tool for shedding light on the basic biology of this recently identified cholesterol excretion pathway. However, enhancing TICE as well as macrophage RCT may also partially account for the anti-atherogenic and anti-inflammatory effects of 4F. The details regarding the mechanism by which 4F enhances TICE, as well as the connections between TICE and atherosclerosis and other systemic inflammatory disorders, are the subjects of ongoing investigations in our laboratory.

REFERENCES

1. Papa, A., S. Danese, R. Urgesi, A. Grillo, S. Guglielmo, I. Roberto, M. Bonizzi, L. Guidi, I. De Vitis, A. Santoliquido, et al. 2006. Early atherosclerosis in patients with inflammatory bowel disease. *Eur. Rev. Med. Pharmacol. Sci.* **10:** 7–11.

2. Yarur, A. J., A. R. Deshpande, D. M. Pechman, L. Tamariz, M. T. Abreu, and D. A. Sussman. 2011. Inflammatory bowel disease is associated with an increased incidence of cardiovascular events. *Am. J. Gastroenterol.* **106:** 741–747.

3. van Leuven, S. I., R. Hezemans, J. H. Levels, S. Snoek, P. C. Stokkers, G. K. Hovingh, J. J. Kastelein, E. S. Stroes, E. de Groot, and D. W. Hommes. 2007. Enhanced atherogenesis and altered high density lipoprotein in patients with Crohn's disease. *J. Lipid Res.* **48:** 2640–2646.

4. Navab, M., G. Hough, G. M. Buga, F. Su, A. C. Wagner, D. Meriwether, A. Chattopadhyay, F. Gao, V. Grijalva, J. S. Danciger, et al. 2013. Transgenic 6F tomatoes act on the small intestine to prevent systemic inflammation and dyslipidemia caused by Western diet and intestinally derived lysophosphatidic acid. *J. Lipid Res.* **54:** 3403–3418.

5. Navab, M., S. T. Reddy, G. M. Anantharamaiah, G. Hough, G. M. Buga, J. Danciger, and A. M. Fogelman. 2012. D-4F-mediated reduction in metabolites of arachidonic and linoleic acids in the small intestine is associated with decreased inflammation in low-density lipoprotein receptor-null mice. *J. Lipid Res.* **53:** 437–445.

6. Navab, M., A. Chattopadhyay, G. Hough, D. Meriwether, S. I. Fogelman, A. C. Wagner, V. Grijalva, F. Su, G. M. Anantharamaiah, L. H. Hwang, et al. 2015. Source and role of intestinally derived lysophosphatidic acid in dyslipidemia and atherosclerosis. *J. Lipid Res.* **56:** 871–887.

7. Chattopadhyay, A., M. Navab, G. Hough, F. Gao, D. Meriwether, V. Grijalva, J. R. Springstead, M. N. Palgnachari, R. Namiri-Kalantari, F. Su, et al. 2013. A novel approach to oral apoA-I mimetic therapy. *J. Lipid Res.* **54:** 995–1010. [Erratum. 2013. *J. Lipid Res.* 54: 3220.]

8. Brunham, L. R., and M. R. Hayden. 2015. Human genetics of HDL: insight into particle metabolism and function. *Prog. Lipid Res.* **58:** 14–25.

9. Brunham, L. R., J. K. Kruit, J. Iqbal, C. Fievet, J. M. Timmins, T. D. Pape, B. A. Coburn, N. Bissada, B. Staels, A. K. Groen, et al. 2006. Intestinal ABCA1 directly contributes to HDL biogenesis in vivo. *J. Clin. Invest.* **116:** 1052–1062.

10. Barter, P. J., S. Nicholls, K. A. Rye, G. M. Anantharamaiah, M. Navab, and A. M. Fogelman. 2004. Antiinflammatory properties of HDL. *Circ. Res.* **95:** 764–772.

11. Navab, M., J. A. Berliner, G. Subbanagounder, S. Hama, A. J. Lusis, L. W. Castellani, S. Reddy, D. Shih, W. Shi, A. D. Watson, et al. 2001. HDL and the inflammatory response induced by LDL-derived oxidized phospholipids. *Arterioscler. Thromb. Vasc. Biol.* **21:** 481–488.

12. Christison, J., A. Karjalainen, J. Brauman, F. Bygrave, and R. Stocker. 1996. Rapid reduction and removal of HDL- but not LDL-associated cholesteryl ester hydroperoxides by rat liver perfused in situ. *Biochem. J.* **314:** 739–742.

13. Shao, B., and J. W. Heinecke. 2009. HDL, lipid peroxidation, and atherosclerosis. *J. Lipid Res.* **50:** 599–601.

14. Yvan-Charvet, L., N. Wang, and A. R. Tall. 2010. Role of HDL, ABCA1, and ABCG1 transporters in cholesterol efflux and immune responses. *Arterioscler. Thromb. Vasc. Biol.* **30:** 139–143.

15. Chau, P., Y. Nakamura, C. J. Fielding, and P. E. Fielding. 2006. Mechanism of prebeta-HDL formation and activation. *Biochemistry.* **45:** 3981–3987.

16. Birner-Gruenberger, R., M. Schittmayer, M. Holzer, and G. Marsche. 2014. Understanding high-density lipoprotein function in disease: recent advances in proteomics unravel the complexity of its composition and biology. *Prog. Lipid Res.* **56:** 36–46.

17. Tall, A. R., L. Yvan-Charvet, M. Westerterp, and A. J. Murphy. 2012. Cholesterol efflux: a novel regulator of myelopoiesis and atherogenesis. *Arterioscler. Thromb. Vasc. Biol.* **32:** 2547–2552.

18. Navab, M., S. Y. Hama, G. P. Hough, G. Subbanagounder, S. T. Reddy, and A. M. Fogelman. 2001. A cell-free assay for detecting HDL that is dysfunctional in preventing the formation of or inactivating oxidized phospholipids. *J. Lipid Res.* **42:** 1308–1317.

19. Navab, M., S. Y. Hama, C. J. Cooke, G. M. Anantharamaiah, M. Chaddha, L. Jin, G. Subbanagounder, K. F. Faull, S. T. Reddy, N. E. Miller, et al. 2000. Normal high density lipoprotein inhibits three steps in the formation of mildly oxidized low density lipoprotein: ste. *J. Lipid Res.* **41:** 1481–1494.

20. Bergt, C., S. Pennathur, X. Fu, J. Byun, K. O'Brien, T. O. McDonald, P. Singh, G. M. Anantharamaiah, A. Chait, J. Brunzell, et al. 2004. The myeloperoxidase product hypochlorous acid oxidizes HDL in the human artery wall and impairs ABCA1-dependent cholesterol transport. *Proc. Natl. Acad. Sci. USA.* **101:** 13032–13037.

21. Boughton-Smith, N. K., J. L. Wallace, and B. J. R. Whitle. 1988. Relationship between arachidonic acid metabolism, myeloperoxidase activity and leukocyte infiltration in a rat model of inflammatory bowel disease. *Agents Actions.* **25:** 115–123.

22. Tall, A. R. 2008. Cholesterol efflux pathways and other potential mechanisms involved in the athero-protective effect of high density lipoproteins. *J. Intern. Med.* **263:** 256–273.

23. Hong, C., and P. Tontonoz. 2014. Liver X receptors in lipid metabolism: opportunities for drug discovery. *Nat. Rev. Drug Discov.* **13:** 433–444.

24. Vrins, C. L. 2010. From blood to gut: direct secretion of cholesterol via transintestinal cholesterol efflux. *World J. Gastroenterol.* **16:** 5953–5957.

25. van der Velde, A. E., G. Brufau, and A. K. Groen. 2010. Transintestinal cholesterol efflux. *Curr. Opin. Lipidol.* **21:** 167–171.

26. Temel, R. E., and J. M. Brown. 2010. A new framework for reverse cholesterol transport: non-biliary contributions to reverse cholesterol transport. *World J. Gastroenterol.* **16:** 5946–5952.

27. Brufau, G., A. K. Groen, and F. Kuipers. 2011. Reverse cholesterol transport revisited: contribution of biliary versus intestinal cholesterol excretion. *Arterioscler. Thromb. Vasc. Biol.* **31:** 1726–1733.

28. Temel, R. E., and J. M. Brown. 2012. Biliary and nonbiliary contributions to reverse cholesterol transport. *Curr. Opin. Lipidol.* **23:** 85–90.

29. van der Veen, J. N., T. H. van Dijk, C. L. Vrins, H. van Meer, R. Havinga, K. Bijsterveld, U. J. Tietge, A. K. Groen, and F. Kuipers. 2009. Activation of the liver X receptor stimulates trans-intestinal excretion of plasma cholesterol. *J. Biol. Chem.* **284:** 19211–19219.

30. Kruit, J. K., T. Plosch, R. Havinga, R. Boverhof, P. H. Groot, A. K. Groen, and F. Kuipers. 2005. Increased fecal neutral sterol loss upon liver X receptor activation is independent of biliary sterol secretion in mice. *Gastroenterology.* **128:** 147–156.

31. Temel, R. E., W. Tang, Y. Ma, L. L. Rudel, M. C. Willingham, Y. A. Ioannou, J. P. Davies, L. M. Nilsson, and L. Yu. 2007. Hepatic Niemann-Pick C1-like 1 regulates biliary cholesterol concentration and is a target of ezetimibe. *J. Clin. Invest.* **117:** 1968–1978.

32. Temel, R. E., J. K. Sawyer, L. Yu, C. Lord, C. Degirolamo, A. McDaniel, S. Marshall, N. Wang, R. Shah, L. L. Rudel, et al. 2010. Biliary sterol secretion is not required for macrophage reverse cholesterol transport. *Cell Metab.* **12:** 96–102.

33. Morrone, D., W. S. Weintraub, P. P. Toth, M. E. Hanson, R. S. Lowe, J. Lin, A. K. Shah, and A. M. Tershakovec. 2012. Lipid-altering efficacy of ezetimibe plus statin and statin monotherapy and identification of factors associated with treatment response: a pooled analysis of over 21,000 subjects from 27 clinical trials. *Atherosclerosis.* **223:** 251–261.

34. Grünhage, F., M. Acalovschi, S. Tirziu, M. Walier, T. F. Wienker, A. Ciocan, O. Mosteanu, T. Sauerbruch, and F. Lammert. 2007. Increased gallstone risk in humans conferred by common variant of hepatic ATP-binding cassette transporter for cholesterol. *Hepatology.* **46:** 793–801.

35. Venkatachalapathi, Y. V., M. C. Phillips, R. M. Epand, R. F. Epand, E. M. Tytler, J. P. Segrest, and G. M. Anantharamaiah. 1993. Effect of end group blockage on the properties of a class A amphipathic helical peptide. *Proteins.* **15:** 349–359.

36. Getz, G. S., G. D. Wool, and C. A. Reardon. 2009. Apoprotein A-I mimetic peptides and their potential anti-atherogenic mechanisms of action. *Curr. Opin. Lipidol.* **20:** 171–175.

37. Van Lenten, B. J., A. C. Wagner, M. Navab, G. M. Anantharamaiah, S. Hama, S. T. Reddy, and A. M. Fogelman. 2007. Lipoprotein inflammatory properties and serum amyloid A levels but not cholesterol levels predict lesion area in cholesterol-fed rabbits. *J. Lipid Res.* **48:** 2344–2353.

38. Navab, M., G. M. Anantharamaiah, S. T. Reddy, and A. M. Fogelman. 2006. Apolipoprotein A-I mimetic peptides and their role in atherosclerosis prevention. *Nat. Clin. Pract. Cardiovasc. Med.* **3:** 540–547.

39. Sherman, C. B., S. J. Peterson, and W. H. Frishman. 2010. Apolipoprotein A-I mimetic peptides: a potential new therapy for the prevention of atherosclerosis. *Cardiol. Rev.* **18:** 141–147.

40. Navab, M., G. M. Anantharamaiah, S. T. Reddy, B. J. Van Lenten, B. J. Ansell, and A. M. Fogelman. 2006. Mechanisms of disease:

proatherogenic HDL—an evolving field. *Nat. Clin. Pract. Endocrinol. Metab.* **2:** 504–511.

41. Bloedon, L. T., R. Dunbar, D. Duffy, P. Pinell-Salles, R. Norris, B. J. DeGroot, R. Movva, M. Navab, A. M. Fogelman, and D. J. Rader. 2008. Safety, pharmacokinetics, and pharmacodynamics of oral apoA-I mimetic peptide D-4F in high-risk cardiovascular patients. *J. Lipid Res.* **49:** 1344–1352.

42. Navab, M., S. T. Reddy, B. J. Van Lenten, G. M. Buga, G. Hough, A. C. Wagner, and A. M. Fogelman. 2012. High-density lipoprotein and 4F peptide reduce systemic inflammation by modulating intestinal oxidized lipid metabolism: novel hypotheses and review of literature. *Arterioscler. Thromb. Vasc. Biol.* **32:** 2553–2560.

43. Rosenbaum, M. A., P. Chaudhuri, B. Abelson, B. N. Cross, and L. M. Graham. 2015. Apolipoprotein A-I mimetic peptide reverses impaired arterial healing after injury by reducing oxidative stress. *Atherosclerosis.* **241:** 709–715.

44. Meriwether, D., S. Imaizumi, V. Grijalva, G. Hough, L. Vakili, G. M. Anantharamaiah, R. Farias-Eisner, M. Navab, A. M. Fogelman, S. T. Reddy, et al. 2011. Enhancement by LDL of transfer of L-4F and oxidized lipids to HDL in C57BL/6J mice and human plasma. *J. Lipid Res.* **52:** 1795–1809.

45. Navab, M., I. Shechter, G. M. Anantharamaiah, S. T. Reddy, B. J. Van Lenten, and A. M. Fogelman. 2010. Structure and function of HDL mimetics. *Arterioscler. Thromb. Vasc. Biol.* **30:** 164–168.

46. Navab, M., S. T. Reddy, G. M. Anantharamaiah, S. Imaizumi, G. Hough, S. Hama, and A. M. Fogelman. 2011. Intestine may be a major site of action for the apoA-I mimetic peptide 4F whether administered subcutaneously or orally. *J. Lipid Res.* **52:** 1200–1210.

47. Deleted in proof.

48. Vrins, C. L. J., R. Ottenhoff, K. van den Oever, D. R. de Waart, J. K. Kruyt, Y. Zhao, T. J. C. van Berkel, L. M. Havekes, J. M. Aerts, M. van Eck, et al. 2012. Trans-intestinal cholesterol efflux is not mediated through high density lipoprotein. *J. Lipid Res.* **53:** 2017–2023.

49. Le May, C., J. M. Berger, A. Lespine, B. Pillot, X. Prieur, E. Letessier, M. M. Hussain, X. Collet, B. Cariou, and P. Costet. 2013. Transintestinal cholesterol excretion is an active metabolic process modulated by PCSK9 and statin involving ABCB1. *Arterioscler. Thromb. Vasc. Biol.* **33:** 1484–1493.

50. Van Lenten, B. J., A. C. Wagner, C. L. Jung, P. Ruchala, A. J. Waring, R. I. Lehrer, A. D. Watson, S. Hama, M. Navab, G. M. Anantharamaiah, et al. 2008. Anti-inflammatory apoA-I-mimetic peptides bind oxidized lipids with much higher affinity than human apoA-I. *J. Lipid Res.* **49:** 2302–2311.

51. Jones, M. K., G. M. Anantharamaiah, and J. P. Segrest. 1992. Computer programs to identify and classify amphipathic alpha helical domains. *J. Lipid Res.* **33:** 287–296.

52. Palgunachari, M. N., V. K. Mishra, S. Lund-Katz, M. C. Phillips, S. O. Adeyeye, S. Alluri, G. M. Anantharamaiah, and J. P. Segrest. 1996. Only the two end helixes of eight tandem amphipathic helical domains of human apo A-I have significant lipid affinity. Implications for HDL assembly. *Arterioscler. Thromb. Vasc. Biol.* **16:** 328–338.

53. Handattu, S. P., D. W. Garber, D. C. Horn, D. W. Hughes, B. Berno, A. D. Bain, V. K. Mishra, M. N. Palgunachari, G. Datta, G. M. Anantharamaiah, et al. 2007. ApoA-I mimetic peptides with differing ability to inhibit atherosclerosis also exhibit differences in their interactions with membrane bilayers. *J. Biol. Chem.* **282:** 1980–1988.

54. Havel, R. J., H. A. Eder, and J. H. Bragdon. 1955. The distribution and chemical composition of ultracentrifugally separated lipoproteins in human serum. *J. Clin. Invest.* **34:** 1345–1353.

55. Williams, K. J., J. P. Argus, Y. Zhu, M. Q. Wilks, B. N. Marbois, A. G. York, Y. Kidani, A. L. Pourzia, D. Akhavan, D. N. Lisiero, et al. 2013. An essential requirement for the SCAP/SREBP signaling axis to protect cancer cells from lipotoxicity. *Cancer Res.* **73:** 2850–2862.

56. Temel, R. E., R. G. Lee, K. L. Kelley, M. A. Davis, R. Shah, J. K. Sawyer, M. D. Wilson, and L. L. Rudel. 2005. Intestinal cholesterol absorption is substantially reduced in mice deficient in both ABCA1 and ACAT2. *J. Lipid Res.* **46:** 2423–2431.

57. Bligh, E. G., and W. J. Dyer. 1959. A rapid method of total lipid extraction and purification. *Can. J. Biochem. Physiol.* **37:** 911–917.

58. Gerhardt, K. O., C. W. Gehrke, I. T. Rogers, M. A. Flynn, and D. J. Hentges. 1977. Gas-liquid chromatography of fecal neutral steroids. *J. Chromatogr. A.* **135:** 341–349.

59. Folch, J., M. Lees, and G. H. Sloane Stanley. 1957. A simple method for the isolation and purification of total lipides from animal tissues. *J. Biol. Chem.* **226:** 497–509.

60. Chavez-Santoscoy, A. V., L. M. Huntimer, A. E. Ramer-Tait, M. Wannemuehler, and B. Narasimhan. 2012. Harvesting murine alveolar macrophages and evaluating cellular activation induced by polyanhydride nanoparticles. *J. Vis. Exp.* **64:** 3883.

61. Clarke, L. L. 2009. A guide to Ussing chamber studies of mouse intestine. *Am. J. Physiol. Gastrointest. Liver Physiol.* **296:** G1151–G1166.

62. Iqbal, J., and M. M. Hussain. 2005. Evidence for multiple complementary pathways for efficient cholesterol absorption in mice. *J. Lipid Res.* **46:** 1491–1501.

63. Zhang, Y., I. Zanotti, M. P. Reilly, J. M. Glick, G. H. Rothblat, and D. J. Rader. 2003. Overexpression of apolipoprotein A-I promotes reverse transport of cholesterol from macrophages to feces in vivo. *Circulation.* **108:** 661–663.

64. Garcia, Z. C., K. S. Poksay, K. Boström, D. F. Johnson, M. E. Balestra, I. Shechter, and T. L. Innerarity. 1992. Characterization of apolipoprotein B mRNA editing from rabbit intestine. *Arterioscler. Thromb. Vasc. Biol.* **12:** 172–179.

65. Wiedmann, T. S., C. Deye, and D. Kallick. 2001. Interaction of bile salt and phospholipids with bovine submaxillary mucin. *Pharm. Res.* **18:** 45–53.

66. Li, C. Y., C. L. Zimmerman, and T. S. Wiedmann. 1996. Diffusivity of bile salt/phospholipid aggregates in mucin. *Pharm. Res.* **13:** 535–541.

67. Canny, G., A. Swidsinski, and B. A. McCormick. 2006. Interactions of intestinal epithelial cells with bacteria and immune cells: methods to characterize microflora and functional consequences. *Methods Mol. Biol.* **341:** 17–35.

68. Pappenheimer, J. R., M. L. Karnovsky, and J. E. Maggio. 1997. Absorption and excretion of undegradable peptides: role of lipid solubility and net charge. *J. Pharmacol. Exp. Ther.* **280:** 292–300.

69. Torjman, M. C., J. I. Joseph, C. Munsick, M. Morishita, and Z. Grunwald. 2005. Effects of isoflurane on gastrointestinal motility after brief exposure in rats. *Int. J. Pharm.* **294:** 65–71.

70. van der Velde, A. E., C. L. Vrins, K. van den Oever, I. Seemann, R. P. Oude Elferink, M. van Eck, F. Kuipers, and A. K. Groen. 2008. Regulation of direct transintestinal cholesterol excretion in mice. *Am. J. Physiol. Gastrointest. Liver Physiol.* **295:** G203–G208.

71. Casteleyn, C., A. Rekecki, A. Van der Aa, P. Simoens, and W. Van den Broeck. 2010. Surface area assessment of the murine intestinal tract as a prerequisite for oral dose translation from mouse to man. *Lab. Anim.* **44:** 176–183.

72. Xie, Q., S. P. Zhao, and F. Li. 2010. D-4F, an apolipoprotein A-I mimetic peptide, promotes cholesterol efflux from macrophages via ATP-binding cassette transporter A1. *Tohoku J. Exp. Med.* **220:** 223–228.

73. Nijstad, N., T. Gautier, F. Briand, D. J. Rader, and U. J. Tietge. 2011. Biliary sterol secretion is required for functional in vivo reverse cholesterol transport in mice. *Gastroenterology.* **140:** 1043–1051.

74. Reddy, S. T., M. Navab, G. M. Anantharamaiah, and A. M. Fogelman. 2014. Apolipoprotein A-I mimetics. *Curr. Opin. Lipidol.* **25:** 304–308.

75. Wool, G. D., T. Vaisar, C. A. Reardon, and G. S. Getz. 2009. An apoA-I mimetic peptide containing a proline residue has greater in vivo HDL binding and anti-inflammatory ability than the 4F peptide. *J. Lipid Res.* **50:** 1889–1900.

76. Garrigues, A., A. E. Escargueil, and S. Orlowski. 2002. The multidrug transporter, P-glycoprotein, actively mediates cholesterol redistribution in the cell membrane. *Proc. Natl. Acad. Sci. USA.* **99:** 10347–10352.

77. Dadgostar, A., S. Vazirian, K. Farah, and M. Faraz. 2014. The 4F peptide significantly decreases intestinal oxidized fatty acids. *FASEB J.* **28 (Suppl.):** 835.1.

78. Imaizumi, S., V. Grijalva, M. Navab, B. J. Van Lenten, A. C. Wagner, G. M. Anantharamaiah, A. M. Fogelman, and S. T. Reddy. 2010. L-4F differentially alters plasma levels of oxidized fatty acids resulting in more anti-inflammatory HDL in mice. *Drug Metab. Lett.* **4:** 139–148.

79. Navab, M., G. M. Anantharamaiah, S. T. Reddy, S. Hama, G. Hough, V. R. Grijalva, A. C. Wagner, J. S. Frank, G. Datta, D. Garber, et al. 2004. Oral D-4F causes formation of pre-beta high-density lipoprotein and improves high-density lipoprotein-mediated cholesterol efflux and reverse cholesterol transport from macrophages in apolipoprotein E-null mice. *Circulation.* **109:** 3215–3220.

80. Yancey, P. G., J. K. Bielicki, W. J. Johnson, S. Lund-Katz, M. N. Palgunachari, G. M. Anantharamaiah, J. P. Segrest, M. C. Phillips, and G. H. Rothblat. 1995. Efflux of cellular cholesterol and phospholipid to lipid-free apolipoproteins and class A amphipathic peptides. *Biochemistry.* **34:** 7955–7965.

81. Tang, C., A. M. Vaughan, G. M. Anantharamaiah, and J. F. Oram. 2006. Janus kinase 2 modulates the lipid-removing but not protein-stabilizing interactions of amphipathic helices with ABCA1. *J. Lipid Res.* **47:** 107–114.
82. Bielicki, J. K., H. Zhang, Y. Cortez, Y. Zheng, V. Narayanaswami, A. Patel, J. Johansson, and S. Azhar. 2010. A new HDL mimetic peptide that stimulates cellular cholesterol efflux with high efficiency greatly reduces atherosclerosis in mice. *J. Lipid Res.* **51:** 1496–1503.
83. Xie, P., L. Jia, Y. Ma, J. Ou, H. Miao, N. Wang, F. Guo, A. Yazdanyar, X. C. Jiang, and L. Yu. 2013. Ezetimibe inhibits hepatic Niemann-Pick C1-Like 1 to facilitate macrophage reverse cholesterol transport in mice. *Arterioscler. Thromb. Vasc. Biol.* **33:** 920–925.
84. Ng, D. S. 2004. Insight into the role of LCAT from mouse models. *Rev. Endocr. Metab. Disord.* **5:** 311–318.
85. Lund-Katz, S., B. Hammerschlag, and M. C. Phillips. 1982. Kinetics and mechanism of free cholesterol exchange between human serum high- and low-density lipoproteins. *Biochemistry.* **21:** 2964–2969.
86. Barter, P. J., H. B. Brewer, M. J. Chapman, C. H. Hennekens, D. J. Rader, and A. R. Tall. 2003. Cholesteryl ester transfer protein: a novel target for raising HDL and inhibiting atherosclerosis. *Arterioscler. Thromb. Vasc. Biol.* **23:** 160–167.
87. Briand, F., M. Tréguier, A. André, D. Grillot, M. Issandou, K. Ouguerram, and T. Sulpice. 2010. Liver X receptor activation promotes macrophage-to-feces reverse cholesterol transport in a dyslipidemic hamster model. *J. Lipid Res.* **51:** 763–770.
88. Lo Sasso, G., S. Murzilli, L. Salvatore, I. D'Errico, M. Petruzzelli, P. Conca, Z. Y. Jiang, L. Calabresi, P. Parini, and A. Moschetta. 2010. Intestinal specific LXR activation stimulates reverse cholesterol transport and protects from atherosclerosis. *Cell Metab.* **12:** 187–193.
89. Yasuda, T., D. Grillot, J. T. Billheimer, F. Briand, P. Delerive, S. Huet, and D. J. Rader. 2010. Tissue-specific liver X receptor activation promotes macrophage reverse cholesterol transport in vivo. *Arterioscler. Thromb. Vasc. Biol.* **30:** 781–786.
90. Jakulj, L., J. Besseling, E. S. Stroes, and A. K. Groen. 2013. Intestinal cholesterol secretion: future clinical implications. *Neth. J. Med.* **71:** 459–465.
91. van der Velde, A. E., C. L. Vrins, K. van den Oever, C. Kunne, R. P. Oude Elferink, F. Kuipers, and A. K. Groen. 2007. Direct intestinal cholesterol secretion contributes significantly to total fecal neutral sterol excretion in mice. *Gastroenterology.* **133:** 967–975.
92. Brufau, G., F. Kuipers, Y. Lin, E. A. Trautwein, and A. K. Groen. 2011. A reappraisal of the mechanism by which plant sterols promote neutral sterol loss in mice. *PLoS One.* **6:** e21576.